









TECH BRIEFS

NATIONAL AERONAUTICS AND SPACE ADMINISTRATION

-  **Technology Focus**
-  **Computers/Electronics**
-  **Software**
-  **Materials**
-  **Mechanics**
-  **Machinery/Automation**
-  **Manufacturing**
-  **Bio-Medical**
-  **Physical Sciences**
-  **Information Sciences**
-  **Books and Reports**

INTRODUCTION

Tech Briefs are short announcements of innovations originating from research and development activities of the National Aeronautics and Space Administration. They emphasize information considered likely to be transferable across industrial, regional, or disciplinary lines and are issued to encourage commercial application.

Availability of NASA Tech Briefs and TSPs

Requests for individual Tech Briefs or for Technical Support Packages (TSPs) announced herein should be addressed to

National Technology Transfer Center

Telephone No. (800) 678-6882 or via World Wide Web at www2.nttc.edu/leads/

Please reference the control numbers appearing at the end of each Tech Brief. Information on NASA's Commercial Technology Team, its documents, and services is also available at the same facility or on the World Wide Web at www.nctn.hq.nasa.gov.

Commercial Technology Offices and Patent Counsels are located at NASA field centers to provide technology-transfer access to industrial users. Inquiries can be made by contacting NASA field centers and program offices listed below.

NASA Field Centers and Program Offices

Ames Research Center

Carolina Blake
(650) 604-1754
cblake@mail.arc.nasa.gov

Dryden Flight Research Center

Jenny Baer-Riedhart
(661) 276-3689
jenny.baer-riedhart@dfrc.nasa.gov

Goddard Space Flight Center

Nona Cheeks
(301) 286-5810
Nona.K.Cheeks.1@gssc.nasa.gov

Jet Propulsion Laboratory

Art Murphy, Jr.
(818) 354-3480
arthur.j.murphy-jr@jpl.nasa.gov

Johnson Space Center

Charlene E. Gilbert
(281) 483-3809
commercialization@jsc.nasa.gov

Kennedy Space Center

Jim Aliberti
(321) 867-6224
Jim.Aliberti-1@ksc.nasa.gov

Langley Research Center

Sam Morello
(757) 864-6005
s.a.morello@larc.nasa.gov

John H. Glenn Research Center at Lewis Field

Larry Viterna
(216) 433-3484
cto@grc.nasa.gov

Marshall Space Flight Center

Vernotto McMillan
(256) 544-2615
vernotto.mcmillan@msfc.nasa.gov

Stennis Space Center

Robert Bruce
(228) 688-1929
robert.c.bruce@nasa.gov

NASA Program Offices

At NASA Headquarters there are seven major program offices that develop and oversee technology projects of potential interest to industry:

Carl Ray

Small Business Innovation Research Program (SBIR) & Small Business Technology Transfer Program (STTR)
(202) 358-4652 or
cray@mail.hq.nasa.gov

Dr. Robert Norwood

Office of Commercial Technology (Code RW)
(202) 358-2320 or
rnorwood@mail.hq.nasa.gov

John Mankins

Office of Space Flight (Code MP)
(202) 358-4659 or
jmankins@mail.hq.nasa.gov

Terry Hertz

Office of Aero-Space Technology (Code RS)
(202) 358-4636 or
thertz@mail.hq.nasa.gov

Glen Mucklow

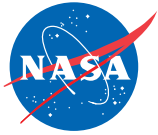
Office of Space Sciences (Code SM)
(202) 358-2235 or
gmucklow@mail.hq.nasa.gov

Roger Crouch

Office of Microgravity Science Applications (Code U)
(202) 358-0689 or
rcrouch@hq.nasa.gov

Granville Paules

Office of Mission to Planet Earth (Code Y)
(202) 358-0706 or
gpaules@mtpe.hq.nasa.gov



TECH BRIEFS

NATIONAL AERONAUTICS AND SPACE ADMINISTRATION



5 Technology Focus: Sensors

- 5 Oxygen-Partial-Pressure Sensor for Aircraft Oxygen Mask
- 5 Three-Dimensional Venturi Sensor for Measuring Extreme Winds
- 6 Swarms of Micron-Sized Sensors
- 7 Monitoring Volcanoes by Use of Air-Dropped Sensor Packages
- 7 Capacitive Sensors for Measuring Masses of Cryogenic Fluids



9 Computers/Electronics

- 9 UHF Microstrip Antenna Array for Synthetic-Aperture Radar
- 10 Multimode Broad-Band Patch Antennas
- 11 164-GHz MMIC HEMT Frequency Doubler
- 11 GPS Position and Heading Circuitry for Ships



13 Software

- 13 Software for Managing Parametric Studies
- 13 Software Aids Visualization of Computed Unsteady Flow
- 13 Software for Testing Electroactive Structural Components
- 13 Advanced Software for Analysis of High-Speed Rolling-Element Bearings
- 14 Web Program for Development of GUIs for Cluster Computers
- 14 XML-Based Generator of C++ Code for Integration With GUIs



15 Materials

- 15 Oxide Protective Coats for Ir/Re Rocket Combustion Chambers
- 15 Simplified Waterproofing of Aerogels
- 16 Improved Thermal-Insulation Systems for Low Temperatures



17 Mechanics

- 17 Device for Automated Cutting and Transfer of Plant Shoots
- 17 Extension of Liouville Formalism to Postinstability Dynamics



19 Machinery/Automation

- 19 Advances in Thrust-Based Emergency Control of an Airplane
- 21 Ultrasonic/Sonic Mechanisms for Drilling and Coring



23 Bio-Medical

- 23 Exercise Device Would Exert Selectable Constant Resistance



25 Physical Sciences

- 25 Improved Apparatus for Measuring Distance Between Axles
- 26 Six Classes of Diffraction-Based Optoelectronic Instruments



27 Information Sciences

- 27 Modernizing Fortran 77 Legacy Codes
- 27 Active State Model for Autonomous Systems



29 Books & Reports

- 29 Shields for Enhanced Protection Against High-Speed Debris
- 29 Scaling of Two-Phase Flows to Partial-Earth Gravity
- 29 Neutral-Axis Springs for Thin-Wall Integral Boom Hinges

This document was prepared under the sponsorship of the National Aeronautics and Space Administration. Neither the United States Government nor any person acting on behalf of the United States Government assumes any liability resulting from the use of the information contained in this document, or warrants that such use will be free from privately owned rights.



Oxygen-Partial-Pressure Sensor for Aircraft Oxygen Mask

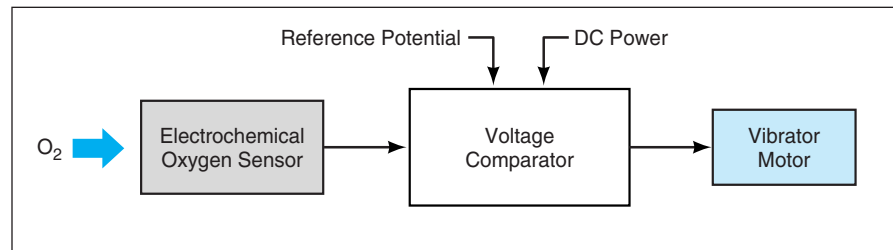
Vibration of the mask against the wearer's nose warns of low oxygen pressure.

Lyndon B. Johnson Space Center, Houston, Texas

A device that generates an alarm when the partial pressure of oxygen decreases to less than a preset level has been developed to help prevent hypoxia in a pilot or other crewmember of a military or other high-performance aircraft. Loss of oxygen partial pressure can be caused by poor fit of the mask or failure of a hose or other component of an oxygen-distribution system. The deleterious physical and mental effects of hypoxia cause the loss of a military aircraft and crew every few years.

The device is installed in the crewmember's oxygen mask and is powered via communication wiring already present in all such oxygen masks. The device (see figure) includes an electrochemical sensor, the output potential of which is proportional to the partial pressure of oxygen. The output of the sensor is amplified and fed to the input of a comparator circuit. A reference potential that corresponds to the amplified sensor output at the alarm oxygen-partial-pressure level is fed to the second input of the comparator. When the sensed partial pressure of oxygen falls below the minimum acceptable level, the output of the comparator goes from the "low" state (a few millivolts) to the "high" state (near the supply potential, which is typically 6.8 V for microphone power).

The switching of the comparator output to the high state triggers a tactile



The **Comparator Triggers the Motor** into operation when the partial pressure of oxygen, measured by the sensor, falls below a preset value represented by the reference potential.

alarm in the form of a vibration in the mask, generated by a small 1.3-Vdc pager motor spinning an eccentric mass at a rate between 8,000 and 10,000 rpm. The sensation of the mask vibrating against the crewmember's nose is very effective at alerting the crewmember, who may already be groggy from hypoxia and is immersed in an environment that is saturated with visual cues and sounds. Indeed, the sensation is one of rudeness, but such rudeness could be what is needed to stimulate the crewmember to take corrective action in a life-threatening situation.

The level chosen for triggering the alarm is the partial pressure of oxygen at an altitude of 11,000 ft (≈ 3.35 km). Because the response time of the electrochemical sensor is about 10 seconds, the device would ordinarily not respond to a sudden but temporary decrease in the partial pressure of oxygen. The device is equipped with a double-pole/double-

throw pushbutton switch for turning on the motor temporarily so that the crewmember can verify that the device has power and the vibrations can be felt. When the alarm has been triggered by low oxygen partial pressure, cycling the same pushbutton switch causes the motor to be turned off for a short time (about 30 seconds). There is also a locking power switch that the crewmember can use to turn the device off in the event of a system failure that turns on the vibrator motor.

This work was done by Mark Kelly and Donald Pettit of Johnson Space Center. Further information is contained in a TSP (see page 1).

This invention is owned by NASA, and a patent application has been filed. Inquiries concerning nonexclusive or exclusive license for its commercial development should be addressed to the Patent Counsel, Johnson Space Center, (281) 483-0837. Refer to MSC-23309.

Three-Dimensional Venturi Sensor for Measuring Extreme Winds

Advantageous features include ruggedness, rapid response, and high dynamic range.

John F. Kennedy Space Center, Florida

A three-dimensional (3D) Venturi sensor is being developed as a compact, rugged means of measuring wind vectors having magnitudes of as much as 300 mph (134 m/s). This sensor also incorporates auxiliary sensors for measuring temperature from -40 to $+120$ °F (-40 to

$+49$ °C), relative humidity from 0 to 100 percent, and atmospheric pressure from 846 to 1,084 millibar (85 to 108 kPa).

Conventional cup-and-vane anemometers are highly susceptible to damage by both high wind forces and debris, due to their moving parts and large profiles. In

addition, they exhibit slow recovery times contributing to an inaccurately high average-speed reading. Ultrasonic and hot-wire anemometers overcome some of the disadvantages of the cup-and-vane anemometers, but they have other disadvantageous features, includ-



Figure 1. A **Prototype Three-Dimensional Venturi Sensor** is shown here mounted in a wind tunnel for testing at Embry-Riddle Aeronautical University, FL.

ing limited dynamic range and susceptibility to errors caused by external acoustic noise and rain.

In contrast, the novel 3D Venturi sensor is less vulnerable to wind damage because of its smaller profile and ruggedness. Since the sensor has no moving parts, it provides increased reliability and lower maintenance costs. It has faster response and recovery times to changing wind conditions than traditional systems. In addition, it offers wide dynamic range and is expected to be relatively insensitive to rain and acoustic energy.

The Venturi effect in this sensor is achieved by the mirrored double-inflection curve, which is then rotated 360° to create the desired detection surfaces. The curve is optimized to provide a good balance of pressure difference between sensor ports and overall maximum fluid velocity while in the shape.

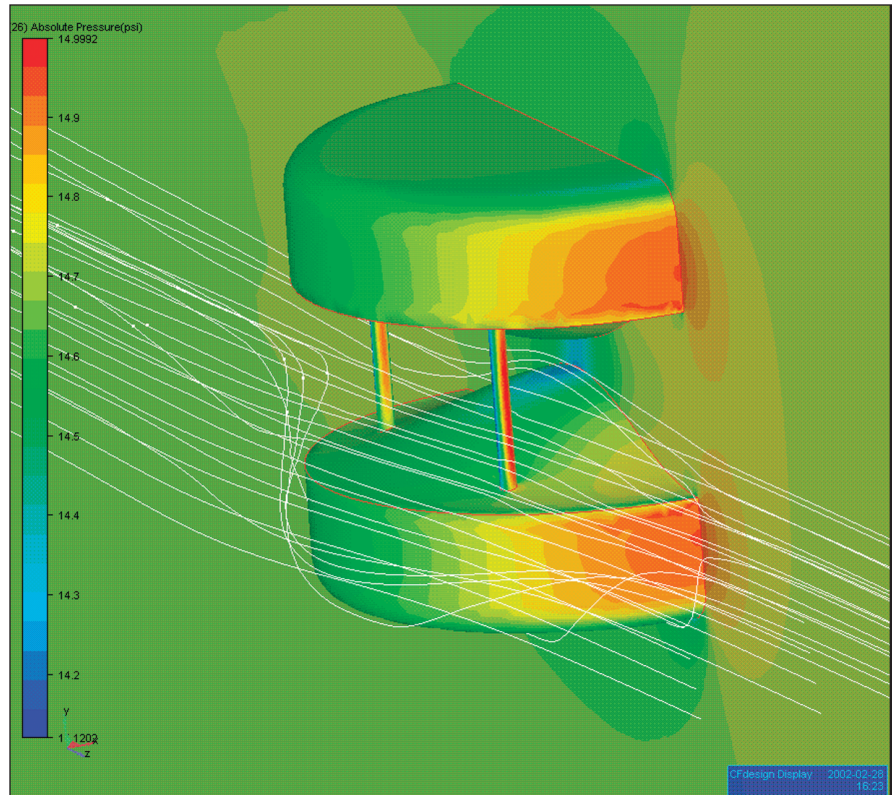


Figure 2. **Pressure and Flow Pattern Results** from simulation of the prototype 3D Venturi sensor are shown at 100-mph (45-m/s) wind velocity.

Four posts are used to separate the two shapes, and their size and location were chosen to minimize effects on the pressure measurements.

The 3D Venturi sensor has smart software algorithms to map the wind pressure exerted on the surfaces of the design. Using Bernoulli's equation, the speed of the wind is calculated from the differences among the pressure readings at the various ports. The direction of the wind is calculated from the spatial distribution and magnitude of the pres-

sure readings. All of the pressure port sizes and locations have been optimized to minimize measurement errors and to reside in areas demonstrating a stable pressure reading proportional to the velocity range.

This work was done by Jan A. Zysko, Jose M. Perotti, and Christopher Amis of Kennedy Space Center and John Randazzo, Norman Blalock, and Anthony Eckhoff of Dynacs, Inc. Further information is contained in a TSP (see page 1). KSC-12435

Swarms of Micron-Sized Sensors

NASA's Jet Propulsion Laboratory, Pasadena, California

A paper presents the concept of swarms of micron-sized and smaller carriers of sensing equipment, denoted generally as controllable granular matter, to be used in exploring remote planets and interplanetary space. The design and manufacture of controllable granular matter would exploit advances in microelectromechanical systems and nanotechnology. Depending on specific designs and applications, controllable granular matter could have characteristics like those of powders, sands, or

aerosols, which would be dispersed into the environments to be explored: For example, sensory grains could be released into orbit around a planet, spread out over ground, or dispersed into wind or into a body of liquid. The grains would thus become integral parts of multiphase environments, where they would function individually and/or collectively to gather information about the environments. In cases of clouds of grains dispersed in outer space, it may be feasible to use laser beams to shape

the clouds to perform specific functions. To enable the full utilization of controllable granular matter, it is necessary to advance the knowledge of the dynamics and controllable characteristics of both individual grains and the powders, sands, or aerosols of which they are parts.

This work was done by Marco Quadrelli of Caltech for NASA's Jet Propulsion Laboratory. Further information is contained in a TSP (see page 1). NPO-30708

Monitoring Volcanoes by Use of Air-Dropped Sensor Packages

Use of these packages would contribute to understanding and prediction of eruptions.

NASA's Jet Propulsion Laboratory, Pasadena, California

Sensor packages that would be dropped from airplanes have been proposed for pre-eruption monitoring of physical conditions on the flanks of awakening volcanoes. The purpose of such monitoring is to gather data that could contribute to understanding and prediction of the evolution of volcanic systems.

Each sensor package, denoted a volcano monitoring system (VMS), would include a housing with a parachute attached at its upper end and a crushable-foam impact absorber at its lower end (see figure). The housing would contain

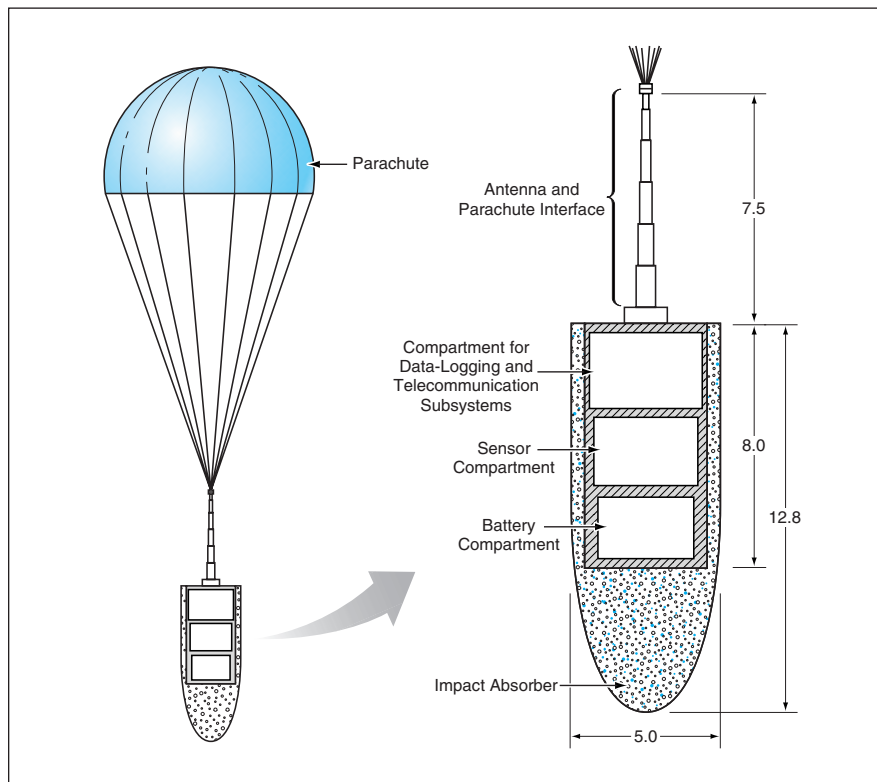
survivable low-power instrumentation that would include a Global Positioning System (GPS) receiver, an inclinometer, a seismometer, a barometer, a thermometer, and CO₂ and SO₂ analyzers. The housing would also contain battery power, control, data-logging, and telecommunication subsystems. The proposal for the development of the VMS calls for the use of commercially available sensor, power, and telecommunication equipment, so that efforts could be focused on integrating all of the equipment into a system that could survive impact

and operate thereafter for 30 days, transmitting data on the pre-eruptive state of a target volcano to a monitoring center.

In a typical scenario, VMSs would be dropped at strategically chosen locations on the flanks of a volcano once the volcano had been identified as posing a hazard from any of a variety of observations that could include eyewitness reports, scientific observations from positions on the ground, synthetic-aperture-radar scans from aircraft, and/or remote sensing from aboard spacecraft. Once dropped, the VMSs would be operated as a network of *in situ* sensors that would transmit data to a local monitoring center. This network would provide observations as part of an integrated volcano-hazard-assessment strategy that would involve both remote sensing and timely observations from the *in situ* sensors.

A similar strategy that involves the use of portable sensors (but not dropping of sensors from aircraft) is already in use in the Volcano Disaster Assistance Program (VDAP), which was developed by the U. S. Geological Survey and the U. S. Office of Foreign Disaster Assistance to respond to volcanic crises around the world. The VMSs would add a greatly needed capability that would enable VDAP response teams to deploy their volcano-monitoring equipment in a more timely manner with less risk to personnel in the field.

This work was done by Sharon Kedar, Tommaso Rivellini, Frank Webb, Brent Blaes, and Caroline Bracho of Caltech and Andrew Lockhart and Ken McGee of the USGS for NASA's Jet Propulsion Laboratory. For further information, access the Technical Support Package (TSP) free on-line at www.techbriefs.com/tsp under the Computers/Electronics category. NPO-30827



A Volcano Monitoring System would be a package of integrated instrumentation that would be dropped on the flanks of a volcano believed to be about to erupt. The dimensions shown here are in inches and are tentative.

Capacitive Sensors for Measuring Masses of Cryogenic Fluids

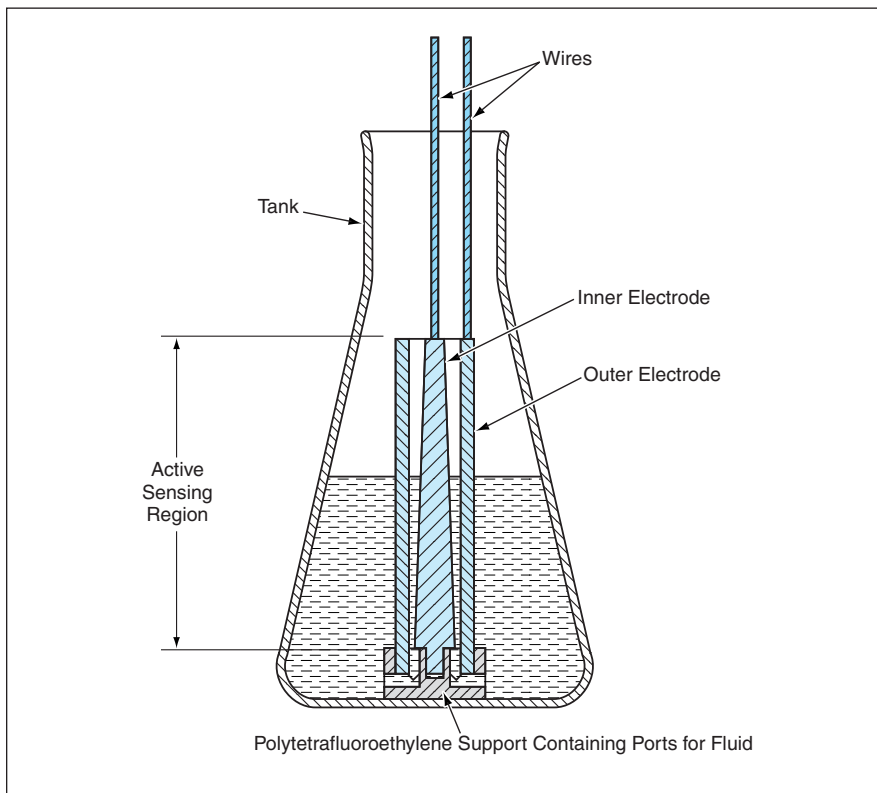
A single capacitance reading is linearly related to the mass of fluid in a tank.

John F. Kennedy Space Center, Florida

An effort is under way to develop capacitive sensors for measuring the masses of cryogenic fluids in tanks. These sensors are intended to function

in both microgravitational and normal gravitational settings, and should not be confused with level sensors, including capacitive ones. A sensor of this type is

conceptually simple in the sense that (1) it includes only one capacitor and (2) if properly designed, its single capacitance reading should be readily convertible to



The Inner Electrode of the Capacitor is tapered so that along with the horizontal-plane cross-sectional area, the capacitance per unit height of the electrodes varies with height.

a close approximation of the mass of the cryogenic fluid in the tank.

Consider a pair of electrically insulated electrodes used as a simple capacitive sensor. In general, the capacitance is proportional to the permittivity of the dielectric medium (in this case, a cryogenic fluid) between the electrodes. The success of design and operation of a sensor of the present type depends on the accuracy of the assumption that to a close approximation, the permittivity of the cryogenic fluid varies linearly with the density of the

fluid. Data on liquid nitrogen, liquid oxygen, and liquid hydrogen, reported by the National Institute of Standards and Technology, indicate that the permittivities and densities of these fluids are, indeed, linearly related to within a few tenths of a percent over the pressure and temperature regions of interest. Hence, ignoring geometric effects for the moment, the capacitance between two electrodes immersed in the fluid should vary linearly with the density, and, hence, with the mass of the fluid.

Of course, it is necessary to take account of the tank geometry. Because most cryogenic tanks do not have uniform cross sections, the readings of level sensors, including capacitive ones, are not linearly correlated with the masses of fluids in the tanks. In a sensor of the present type, the capacitor electrodes are shaped so that at a given height, the capacitance per unit height is approximately proportional to the cross-sectional area of the tank in the horizontal plane at that height (see figure). This shaping should ensure that the contribution of the fluid at each height to the overall capacitance is proportional to the density of fluid at that height, whether the fluid is pulled down by normal gravitation or becomes stratified in microgravitation.

The feasibility of this sensor concept was demonstrated in an experiment in which a simple cylindrical capacitor was immersed in liquid nitrogen and capacitance readings were taken and correlated with mass readings as the liquid nitrogen boiled off. The results of this experiment, taken together with theoretical calculations, have been interpreted as signifying that suitably designed sensors of this type can be expected to yield mass readings accurate to within about one percent of their full-scale values.

This work was done by Mark Nurge and Robert Youngquist of Kennedy Space Center. Further information is contained in a TSP (see page 1).

This invention is owned by NASA, and a patent application has been filed. Inquiries concerning nonexclusive or exclusive license for its commercial development should be addressed to the Technology Programs and Commercialization Office, Kennedy Space Center, (321) 867-8130. Refer to KSC-12457.



UHF Microstrip Antenna Array for Synthetic-Aperture Radar

This antenna performs well over an unusually broad range of frequencies.

NASA's Jet Propulsion Laboratory, Pasadena, California

An ultra-high-frequency microstrip-patch antenna has been built for use in airborne synthetic-aperture radar (SAR). The antenna design satisfies requirements specific to the GeoSAR program, which is dedicated to the development of a terrain-mapping SAR system that can provide information on geology, seismicity, vegetation, and other terrain-related topics. One of the requirements is for ultra-wide-band performance: the antenna must be capable of operating with dual linear polarization in the frequency range of 350 ± 80 MHz, with a peak gain of 10 dB at the middle frequency of 350 MHz and a gain of at least 8 dB at the upper and lower ends (270 and 430 MHz) of the band. Another requirement is compactness: the antenna must fit in the wingtip pod of a Gulfstream II airplane.

The antenna includes a linear array of microstrip-patch radiating elements supported over square cavities. Each patch is square (except for small corner cuts) and has a small square hole at its center. Figure 1 shows the layout and principal dimensions of the cavities and microstrip patches. Wide-band performance is made possible by the relatively large cavity depth.

Each patch is fed by four identical probes positioned symmetrically on the

orthogonal patch axes. To obtain either or both of two orthogonal polarizations, the antenna is fed through either or both of two orthogonal ports. A high degree of isolation between the ports is achieved in the following way: the two probes on opposite sides of the center on same axis are fed 180° out of phase with each other. The electromagnetic fields from these probes travel to the orthogonal probes, but they result in little or no coupling to the orthogonal probes because they cancel each other by virtue of the 180° phase relationship.

As is usual for microstrip devices with thick dielectric substrates (in this case, the cavities are the dielectric substrates) each microstrip patch in this antenna presents undesired inductance at its feed points. With the help of empirical tuning, the feed probes (see Figure 2) are uniquely designed to provide enough capacitance to cancel this inductance. Each feed probe includes an outer metal cylinder plus an inner metal cylinder with a cone at one end. The upper end of the feed probe is separated from the microstrip patch by a 2-mm-thick polytetrafluoroethylene disk. The polytetrafluoroethylene-filled gaps and the cone at one end of the inner

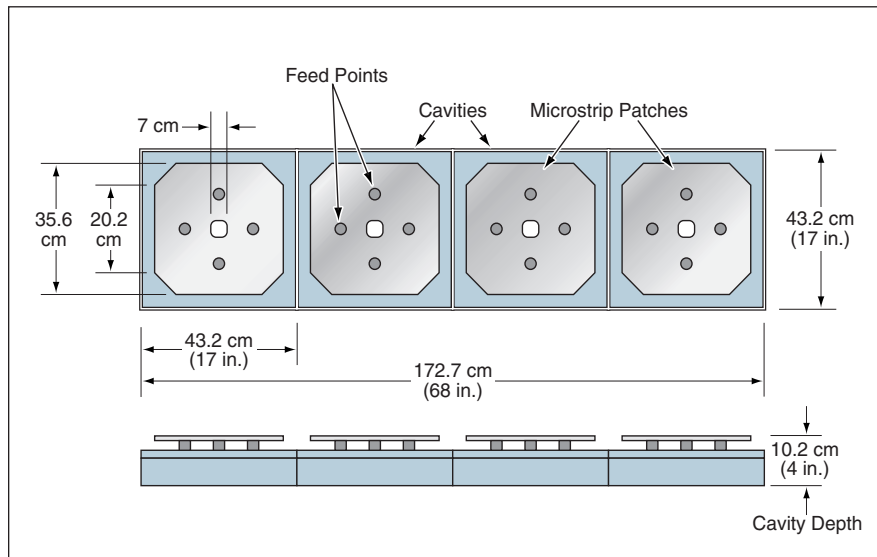


Figure 1. A Linear Array of Microstrip Patches supported over square cavities is shaped and dimensioned to provide the desired gain and broad-band frequency response with dual linear polarization.

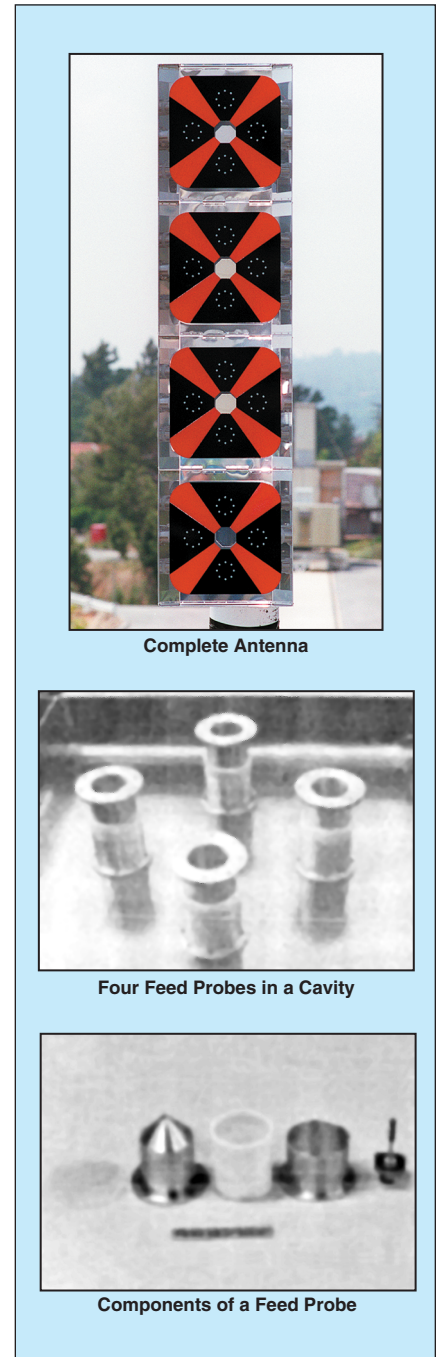


Figure 2. The Feed Probes provide capacitance that counteracts the inductance associated with the depth of the cavity. In addition, the combination of position and phase relationships among the probes is such as to minimize undesired coupling between orthogonal pairs of the probes.

cylinder provide the needed capacitance.

In a test, the antenna exhibited gains of 8, 10, and 11 dB at 270, 350, and 430 MHz, respectively. The 10-dB gain at the middle frequency is associated with an aperture efficiency of 80 percent. This

high aperture efficiency is expected because in the 270-to-430-MHz frequency band, one expects low insertion losses in a power divider, cables, and hybrids that are parts of the antenna feed. Also determined in the tests was the level of isolation between orthogonal ports; this

level was found to be 37 dB across the frequency band.

This work was done by Robert F. Thomas and John Huang of Caltech for NASA's Jet Propulsion Laboratory. Further information is contained in a TSP (see page 1). NPO-20524

Multimode Broad-Band Patch Antennas

Tuning ranges could be octaves wide.

John H. Glenn Research Center, Cleveland, Ohio

Microstrip patch antennas of a proposed type would be tunable over broad wavelength ranges. These antennas would be attractive for use in a variety of microwave communication systems in which there are requirements for transmission and/or reception at multiple, widely separated frequencies.

Prior efforts to construct tunable microstrip patch antennas have involved integration of microstrip circuitry with, variously, ferrite films with magnetic-field tuning, solid-state electronic tuning devices, or piezoelectric tuning actuators. Those efforts have been somewhat successful, but have yielded tuning ranges of 20 percent and smaller — much smaller than needed in typical practical cases.

Like prior microstrip patch antennas (both tunable and non-tunable), the proposed antennas would have instantaneous bandwidths of about 1 percent of their nominal or resonance frequencies. However, these would be tunable over much broader frequency ranges — as much as several octaves, depending on specific designs. They could be fabricated relatively simply and inexpensively by use of conventional photolithography, and without need for integration with solid-state electronic or piezoelectric control devices.

An antenna as proposed (see figure) would include a microstrip patch radiating element on a thin ferroelectric film on a semiconductor substrate with a ground-plane conductor on the underside of the substrate. The ferroelectric film could be, for example, SrTiO₃ with a thickness of the order of 1 or 2 μm.

To enable operation at multiple desired frequencies, the antenna would be designed to resonate in a fundamental TM₀₁ mode that lies at an odd common denominator of the desired frequencies. (In an odd mode, the an-

tenna would radiate strongly in a direction perpendicular to the antenna plane, while an even mode would place a null of the radiation pattern in the perpendicular direction.)

A simple cavity mathematical model yields the following equation for the resonance frequency of the m, n mode:

$$f_{mn} = (c/2\pi\epsilon_r^{1/2})[(m/w)^2 + (n/l)^2]^{1/2},$$

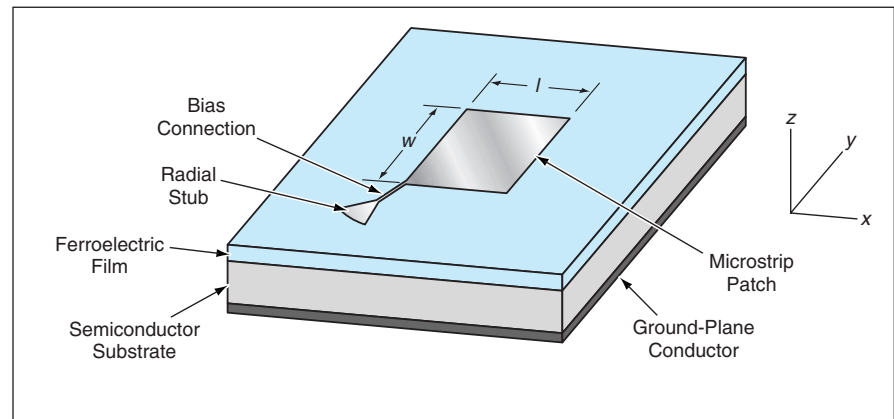
where m and n are integers, c is the speed of light in vacuum, ϵ_r is the effective relative permittivity of the combination of the ferroelectric film and dielectric substrate, and w and l are the width and length of the patch, respectively. In practice, resonance frequencies tend to be somewhat lower than predicted by this simple formula, because of fringing fields.

The value of ϵ_r , and hence the resonance frequency, could be controlled by applying an electric field across the ferroelectric film. For this purpose, a controllable DC bias potential would be applied between the microstrip patch and the ground plane. A virtual ground plane can also be manipulated in this manner by controlling the carrier population in the semiconductor.

Positive bias on the patch forms a sea of electrons near the ferroelectric interface, whereas a reverse bias forms a depletion layer. For isolation of the DC bias source from the radio-frequency signal, the DC bias would be fed in via a high-impedance microstrip transmission line with one end connected to a corner of the patch and the other end terminated in a quarter-wave radial stub (the quarter-wavelength radius would be chosen for a frequency near the middle of the desired radiation-frequency range). A wire would deliver the bias voltage to a radio-frequency virtual-short-circuit location on the transmission line so that the impedance would not be perturbed.

This work was done by Robert R. Romanofsky of Glenn Research Center. Further information is contained in a TSP (see page 1).

Inquiries concerning rights for the commercial use of this invention should be addressed to NASA Glenn Research Center, Commercial Technology Office, Attn: Steve Fedor, Mail Stop 4-8, 21000 Brookpark Road, Cleveland, Ohio 44135. Refer to LEW-16792.



A Multimode Patch Antenna would be designed to resonate at an odd submultiple of possibly widely separated desired operating frequencies. By use of a combination of (1) varying the DC bias voltage to vary the permittivity of the ferroelectric film and (2) selection of the desired harmonic frequency, one could effectively achieve tuning over an unprecedentedly wide frequency range.

164-GHz MMIC HEMT Frequency Doubler

Conversion loss is lower than that of other HEMT frequency doublers above 100 GHz.

NASA's Jet Propulsion Laboratory, Pasadena, California

A monolithic microwave integrated circuit (MMIC) that includes a high-electron-mobility transistor (HEMT) has been developed as a prototype of improved frequency doublers for generating signals at frequencies >100 GHz. Sig-

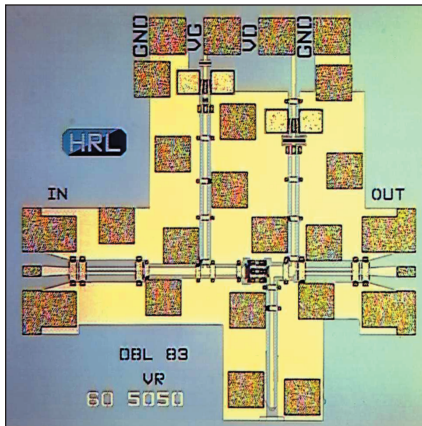


Figure 1. This MMIC HEMT Frequency Doubler occupies a chip with dimensions of 1.1 mm by 1.2 mm by 50 μm .

nal sources that operate in this frequency range are needed for a variety of applications, notably including general radiometry and, more specifically, radiometric remote sensing of the atmosphere.

Heretofore, it has been common practice to use passive (diode-based) frequency multipliers to obtain frequencies >100 GHz. Unfortunately, diode-based frequency multipliers are plagued by high DC power consumption and low conversion efficiency. Moreover, multiplier diodes are not easily integrated with such other multiplier-circuit components as amplifiers and oscillators. The goals of developing the present MMIC HEMT frequency doubler were (1) to utilize the HEMT as an amplifier to increase conversion efficiency (more precisely, to reduce conversion loss), thereby increasing the output power for a given DC power con-

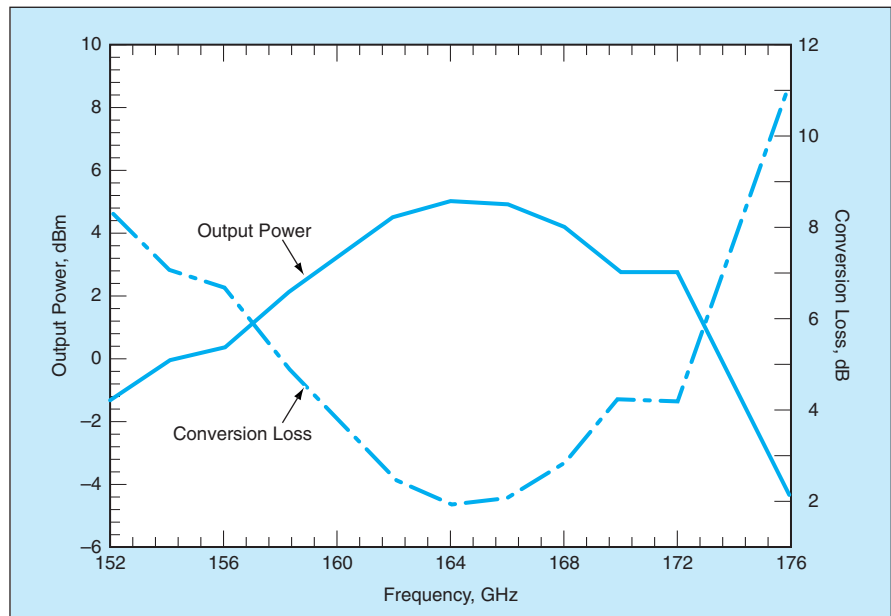


Figure 2. The Output Power and Conversion Loss of the frequency doubler were measured as functions of frequency.

sumption or, equivalently, reducing the DC power consumption for a given output power; and (2) to provide for the integration of amplifier and oscillator components on the same chip.

The MMIC frequency doubler (see Figure 1) contains an AlInAs/GaInAs/InP HEMT biased at pinch-off to make it function as a class-B amplifier (meaning that it conducts in half-cycle pulses). Grounded coplanar waveguides (GCPWs) are used as impedance-matching transmission lines. Air bridges are placed at discontinuities to suppress undesired slot electromagnetic modes. Another combination of GCPWs also serves both as a low-pass filter to suppress undesired oscillations at frequencies below 60 GHz and as a DC blocker. Large decoupling capacitors and epitaxial resistors are added in the drain and gate lines to suppress bias oscillations.

At the output terminal, the fundamental frequency is suppressed by a quarter-wave open stub, which presents a short circuit at the fundamental frequency and an open circuit at the second harmonic.

At an input power of 7 mW, the output power and conversion loss at an output frequency of 164 GHz were found to be 5 dBm (≈ 3.2 mW) and 2 dB, respectively, with a 3-dB output-power bandwidth of 14 GHz. This is the best performance reported to date for an MMIC HEMT frequency doubler above 100 GHz.

This work was done by Lorene Samoska of NASA's Jet Propulsion Laboratory, Vesna Radisic, Miro Micovic, Ming Hu, Paul Janke, Catherine Ngo, and Loi Nguyen of HRL Laboratories, LLC, and Matthew Morgan of Caltech. Further information is contained in a TSP (see page 1). NPO-21197

GPS Position and Heading Circuitry for Ships

Lyndon B. Johnson Space Center, Houston, Texas

Circuit boards that contain radio-frequency (RF) and digital circuitry have been developed by NASA to satisfy a requirement of the Port of Houston Authority for relatively inexpensive Global

Positioning System (GPS) receivers that indicate the azimuthal headings as well as the positions of ships. The receiver design utilizes the unique architecture of the Mitel commercial chip-set, which provides

for an accurate GPS-based heading-determination device. The major components include two RF front ends (each connected to a separate antenna), a surface-acoustic-wave intermediate-frequency fil-

ter between second- and third-stage mixers, a correlator, and a reduced-instruction-set computer. One of the RF front ends operates as a master, the other as a slave. Both RF front ends share a 10-MHz sinusoidal clock oscillator, which provides for more accurate carrier phase measurements between the two antennas. The outputs of the RF front ends are subjected to conventional GPS processing. The com-

mercial-based chip-set design approach provides an inexpensive “open architecture” GPS platform, which can be used in developing and implementing unique GPS-heading and attitude-determination algorithms for specific applications. The heading is estimated from the GPS position solutions of the two antennas by an algorithm developed specifically for this application. If a third (and preferably a

fourth) antenna were added, it would be possible to estimate the attitude of the GPS receiver in three dimensions instead of only its heading in a horizontal plane.

*This work was done by Michael P. Cooke, Hester J. Yim, and Susan F. Gomez of **Johnson Space Center**. Further information is contained in a TSP (see page 1).
MSC-23125*

Software for Managing Parametric Studies

The Information Power Grid Virtual Laboratory (ILab) is a Practical Extraction and Reporting Language (PERL) graphical-user-interface computer program that generates shell scripts to facilitate parametric studies performed on the Grid. ("The Grid" denotes a worldwide network of supercomputers used for scientific and engineering computations involving data sets too large to fit on desktop computers.) Heretofore, parametric studies on the Grid have been impeded by the need to create control language scripts and edit input data files — painstaking tasks that are necessary for managing multiple jobs on multiple computers. ILab reflects an object-oriented approach to automation of these tasks: All data and operations are organized into packages in order to accelerate development and debugging. A "container" or "document" object in ILab, called an "experiment," contains all the information (data and file paths) necessary to define a complex series of repeated, sequenced, and/or branching processes. For convenience and to enable reuse, this object is serialized to and from disk storage. At run time, the current ILab experiment is used to generate required input files and shell scripts, create directories, copy data files, and then both initiate and monitor the execution of all computational processes.

This program was written by Maurice Yarrow, Karen M. McCann, and Adrian DeVivo of Ames Research Center. For further information, access <http://www.nas.nasa.gov/ILab/>.

Inquiries concerning rights for the commercial use of this invention should be addressed to the Patent Counsel, Ames Research Center, (650) 604-5104. Refer to ARC-14649-1.

Software Aids Visualization of Computed Unsteady Flow

Unsteady Flow Analysis Toolkit (UFAT) is a computer program that synthesizes motions of time-dependent flows represented by very large sets of data generated in computational fluid dynamics simulations. Prior to the development of UFAT, it was necessary to rely on static, single-snapshot depictions of time-dependent flows generated by

flow-visualization software designed for steady flows. Whereas it typically takes weeks to analyze the results of a large-scale unsteady-flow simulation by use of steady-flow visualization software, the analysis time is reduced to hours when UFAT is used. UFAT can be used to generate graphical objects of flow visualization results using multi-block curvilinear grids in the format of a previously developed NASA data-visualization program, PLOT3D. These graphical objects can be rendered using FAST, another popular flow visualization software developed at NASA. Flow-visualization techniques that can be exploited by use of UFAT include time-dependent tracking of particles, detection of vortex cores, extractions of stream ribbons and surfaces, and tetrahedral decomposition for optimal particle tracking. Unique computational features of UFAT include capabilities for automatic (batch) processing, restart, memory mapping, and parallel processing. These capabilities significantly reduce analysis time and storage requirements, relative to those of prior flow-visualization software. UFAT can be executed on a variety of supercomputers.

This program was written by David Kao of Ames Research Center and David Kenwright formerly of Computer Sciences Corp. Further information is contained in a TSP (see page 1).

Inquiries concerning rights for the commercial use of this invention should be addressed to the Patent Counsel, Ames Research Center, (650) 604-5104. Refer to ARC-14800.

Software for Testing Electroactive Structural Components

A computer program generates a graphical user interface that, in combination with its other features, facilitates the acquisition and preprocessing of experimental data on the strain response, hysteresis, and power consumption of a multilayer composite-material structural component containing one or more built-in sensor(s) and/or actuator(s) based on piezoelectric materials. This program runs in conjunction with LabVIEW software in a computer-controlled instrumentation system. For a test, a specimen is instrumented with applied-voltage and current sensors and with

strain gauges. Once the computational connection to the test setup has been made via the LabVIEW software, this program causes the test instrumentation to step through specified configurations. If the user is satisfied with the test results as displayed by the software, the user activates an icon on a front-panel display, causing the raw current, voltage, and strain data to be digitized and saved. The data are also put into a spreadsheet and can be plotted on a graph. Graphical displays are saved in an image file for future reference. The program also computes and displays the power and the phase angle between voltage and current.

This program was written by Robert W. Moses, Robert L. Fox, Archie D. Dimery, Robert G. Bryant, and Qamar Shams of Langley Research Center, and William C. White of Wyle Laboratories. Further information is contained in a TSP (see page 1). LAR-16546

Advanced Software for Analysis of High-Speed Rolling-Element Bearings

COBRA-AHS is a package of advanced software for analysis of rigid or flexible shaft systems supported by rolling-element bearings operating at high speeds under complex mechanical and thermal loads. These loads can include centrifugal and thermal loads generated by motions of bearing components. COBRA-AHS offers several improvements over prior commercial bearing-analysis programs: It includes innovative probabilistic fatigue-life-estimating software that provides for computation of three-dimensional stress fields and incorporates stress-based (in contradistinction to prior load-based) mathematical models of fatigue life. It interacts automatically with the ANSYS finite-element code to generate finite-element models for estimating distributions of temperature and temperature-induced changes in dimensions in iterative thermal/dimensional analyses: thus, for example, it can be used to predict changes in clearances and thermal lockup. COBRA-AHS provides an improved graphical user interface that facilitates the iterative cycle of analysis and design by providing analysis results quickly in graphical form, enabling the user to control interactive runs without leaving the program envi-

ronment, and facilitating transfer of plots and printed results for inclusion in design reports. Additional features include roller-edge stress prediction and influence of shaft and housing distortion on bearing performance.

This program was written by J. V. Poplawski, J. H. Rumbarger, S. M. Peters, H. Galatis, and R. Flower of J. V. Poplawski & Associates for Glenn Research Center. For further information, access www.bearingspecialists.com.

Inquiries concerning rights for the commercial use of this invention should be addressed to NASA Glenn Research Center, Commercial Technology Office, Attn: Steve Fedor, Mail Stop 4-8, 21000 Brookpark Road, Cleveland Ohio 44135. Refer to LEW-17390.

Web Program for Development of GUIs for Cluster Computers

WIGLAF (a **W**eb **I**nterface **G**enerator and **L**egacy **A**pplication **F**açade) is a computer program that provides a Web-based, distributed, graphical-user-interface (GUI) framework that can be adapted to any of a broad range of application programs, written in any programming language, that are executed remotely on any cluster computer system. WIGLAF enables the rapid development of a GUI for controlling and monitoring a specific application program running on the cluster and for transferring data to and from the application program. The only prerequisite for the execution of WIGLAF is a Web-browser program on a user's personal computer connected with the cluster via the Internet. WIGLAF has

a client/server architecture: The server component is executed on the cluster system, where it controls the application program and serves data to the client component. The client component is an applet that runs in the Web browser. WIGLAF utilizes the Extensible Markup Language to hold all data associated with the application software, Java to enable platform-independent execution on the cluster system and the display of a GUI generator through the browser, and the Java Remote Method Invocation software package to provide simple, effective client/server networking.

This program was written by Akos Czikmantory, Thomas Cwik, Gerhard Klimeck, Hook Hua, Fabiano Oyafuso, and Edward Vinyard of Caltech for NASA's Jet Propulsion Laboratory. Further information is contained in a TSP (see page 1).

This software is available for commercial licensing. Please contact Don Hart of the California Institute of Technology at (818) 393-3425. Refer to NPO-30842.

XML-Based Generator of C++ Code for Integration With GUIs

An open source computer program has been developed to satisfy a need for simplified organization of structured input data for scientific simulation programs. Typically, such input data are parsed in from a flat American Standard Code for Information Interchange (ASCII) text file into computational data structures. Also typically, when a graphical user interface (GUI) is used,

there is a need to completely duplicate the input information while providing it to a user in a more structured form. Heretofore, the duplication of the input information has entailed duplication of software efforts and increases in susceptibility to software errors because of the concomitant need to maintain two independent input-handling mechanisms. The present program implements a method in which the input data for a simulation program are completely specified in an Extensible Markup Language (XML)-based text file. The key benefit for XML is storing input data in a structured manner. More importantly, XML allows not just storing of data but also describing what each of the data items are. That XML file contains information useful for rendering the data by other applications. It also then generates data structures in the C++ language that are to be used in the simulation program. In this method, all input data are specified in one place only, and it is easy to integrate the data structures into both the simulation program and the GUI. XML-to-C is useful in two ways:

1. As an executable, it generates the corresponding C++ classes and
2. As a library, it automatically fills the objects with the input data values.

This program was written by Hook Hua, Fabiano Oyafuso, and Gerhard Klimeck of Caltech for NASA's Jet Propulsion Laboratory. Further information is contained in a TSP (see page 1).

This software is available for commercial licensing. Please contact Don Hart of the California Institute of Technology at (818) 393-3425. Refer to NPO-30844.



Oxide Protective Coats for Ir/Re Rocket Combustion Chambers

Lyndon B. Johnson Space Center, Houston, Texas

An improved material system has been developed for rocket engine combustion chambers for burning oxygen/hydrogen mixtures or novel monopropellants, which are highly oxidizing at operating temperatures. The baseline for developing the improved material system is a prior iridium/rhenium system for chambers burning nitrogen tetroxide/monomethyl hydrazine mixtures, which are less oxidizing. The baseline combustion chamber comprises an outer layer of rhenium that provides

structural support, plus an inner layer of iridium that acts as a barrier to oxidation of the rhenium. In the improved material system, the layer of iridium is thin and is coated with a thermal fatigue-resistant refractory oxide (specifically, hafnium oxide) that serves partly as a thermal barrier to decrease the temperature and thus the rate of oxidation of the rhenium. The oxide layer also acts as a barrier against the transport of oxidizing species to the surface of the iridium. Tests in which various oxygen/hydrogen

mixtures were burned in iridium/rhenium combustion chambers lined with hafnium oxide showed that the operational lifetimes of combustion chambers of the improved material system are an order of magnitude greater than those of the baseline combustion chambers.

This work was done by Arthur J. Fortini and Robert H. Tuffias of Ultramet for Johnson Space Center. Further information is contained in a TSP (see page 1). MSC-23214

Simplified Waterproofing of Aerogels

Silanization is performed in a single treatment at moderate temperature and pressure.

Ames Research Center, Moffett Field, California

A relatively simple silanization process has been developed for waterproofing or rewaterproofing aerogels, xerogels, and aerogel/tile composites, and other, similar low-density, highly microporous materials. Such materials are potentially attractive for a variety of applications — especially for thermal-insulation panels that are required to be thin and lightweight. Unfortunately, such materials are also hydrophilic and tend to collapse after adsorbing water from the air. Hence, an effective means of waterproofing is necessary to enable practical exploitation of aerogels and the like.

Older processes for waterproofing aerogels are time-consuming, labor-intensive, and expensive, relative to the present process. Each of the older processes includes a number of different chemical-treatment steps, and some include the use of toxic halogenated surface-modifying compounds, pressures as high as hundreds of atmospheres, and/or temperatures as high as 1,000 °C.

In contrast, the present silanization process involves a single step, pressure and temperature near ambient values, and no use of toxic halogenated compounds. In this process, an aerogel object that has been dried and otherwise fully formed is exposed to the vapor(s) of one or more silicon-containing organic com-

Material	Degree of Water Pickup (Percent of Original Weight) by Untreated Sample	Degree of Water Pickup (Percent of Original Weight) by Sample Treated With MDES
Carbon Aerogel	350	1.6
Carbon Xerogel	170	4.8
Carbon-Aerogel/Carbon-Xerogel Composite	280	2.5

Water-Pickup Tests were performed on untreated and treated samples of three microporous materials.

pound(s) at effective concentration(s) in a closed chamber at controlled temperature and pressure. Suitable treatment compounds include silazanes, alkoxy-silanes, and silanes, which react with polar active sites in the aerogel. The temperature need not be particularly high, as long as it is sufficient to sustain vaporization of the treatment compound(s) at the chamber pressure, which typically lies in the range between 76 mm of Hg [0.1 atmosphere (≈ 10 kPa)] and 1.5 m of Hg [≈ 2 atmospheres (≈ 0.2 MPa)].

In one of several experiments, some samples of carbon aerogels, xerogels, and a carbon-aerogel/carbon-xerogel composite were placed in a plastic bag along with an open vial of methyldiethoxysilane (MDES) and the bag was then sealed.

Other samples of the same materials were left untreated. After 24 hours in the bag, the treated samples were shown to have been waterproofed in that they exhibited low degrees of water pickup, whereas the untreated samples showed much higher degrees of water pickup (see table).

This work was done by Ming-Ta S. Hsu, Timothy S. Chen, Susan White, and Daniel J. Rasky of Ames Research Center. Further information is contained in a TSP (see page 1).

This invention is owned by NASA, and a patent application has been filed. Inquiries concerning nonexclusive or exclusive license for its commercial development should be addressed to the Patent Counsel, Ames Research Center, (650) 604-5104. Refer to ARC-14254.

Improved Thermal-Insulation Systems for Low Temperatures

Efficient, robust insulation for soft vacuum.

John F. Kennedy Space Center, Florida

Improved thermal-insulation materials and structures and the techniques for manufacturing them are undergoing development for use in low-temperature applications. Examples of low-temperature equipment for which these thermal insulation systems could provide improved energy efficiency include storage tanks for cryogenics, superconducting electric-power-transmission equipment, containers for transport of food and other perishable commodities, and cold boxes for low-temperature industrial processes. These systems could also be used to insulate piping used to transfer cryogenics and other fluids, such as liquefied natural gas, refrigerants, chilled water, crude oil, or low-pressure steam.

The present thermal-insulation systems are layer composites based partly on the older class of thermal-insulation systems denoted generally as “multilayer insulation” (MLI). A typical MLI structure includes an evacuated jacket, within which many layers of radiation shields are stacked or wrapped close together. Low-thermal-conductivity spacers are typically placed between the reflection layers to keep them from touching. MLI can work very well when a high vacuum level ($<10^{-4}$ torr) is maintained and utmost care is taken during installation, but its thermal performance deteriorates sharply as the pressure in the evacuated space rises into the “soft vacuum” range [pressures >0.1 torr (>13 Pa)]. In addition, the thermal performance of MLI is extremely sensitive to mechanical compression and edge effects and can easily decrease from one to two orders of

magnitude from its ideal value even when the MLI is kept under high vacuum condition.

The present thermal-insulation systems are designed to perform well under soft vacuum level, in particular the range of 1 to 10 torr. They are also designed with larger interlayer spacings to reduce vulnerability to compression (and consequent heat leak) caused by installation and use. The superiority of these systems is the synergistic effect of improvements in materials, design, and manufacture.

The materials used in these systems include combinations of the following:

- Radiation-shielding layers.
- Spacers made of microglass papers or fabrics.
- Granules of either silica or aerogel.
- Outer wrappers that can be made of paper, fabric, or plastic films as required for a given application.

The developmental layered composite insulation systems are divided into the following three categories according to the design structure of the spacer layer:

- Paper, powder deposited on surface of paper, radiation-shielding layer.
- Fabric, powder mechanically deposited inside fabric, radiation-shielding layer.
- Fabric, powder formed chemically within fabric, radiation-shielding layer.

Within each category, thermal-insulation materials may be produced in several different forms of continuous single- or multiple-layer rolls, multiple-layer cylindrical sleeves, and multiple-layer blankets.

The overall effectiveness of the system of insulation depends on thermal performance, versatility and durability, ease of use in manufacturing and installation, and costs of operations and maintenance. Tests of the layered composite insulation systems have thus far confirmed the expectations of high efficiency. Soft-vacuum (1 to 10 torr) systems have much less “vacuum burden” cost compared to high-vacuum (0.00001 torr) systems — the key to lowering manufacturing and life-cycle costs of equipment. Although new systems are targeted for low-cost, soft-vacuum solutions, they also offer advantages for high-vacuum superinsulation applications because of their robust nature. The apparent thermal conductivity for a typical layered composite under evaluation is as follows: 2.4 mW/m-K (milliwatt per meter-kelvin) at 1 torr vacuum level (versus about 12 mW/m-K for MLI) and 0.09 mW/m-K at 10^{-4} torr (comparable to about 0.08 mW/m-K for MLI). These values are for boundary temperatures of approximately 80 and 290 K and residual gas of nitrogen.

This work was done by James E. Fesmire of Kennedy Space Center and Stanislaw D. Augustynowicz of Dynacs Engineering Co. Further information is contained in a TSP (see page 1).

This invention is owned by NASA, and a patent application has been filed. Inquiries concerning nonexclusive or exclusive license for its commercial development should be addressed to the Technology Programs and Commercialization Office, Kennedy Space Center, (321) 867-8130. Refer to KSC-12092.



Device for Automated Cutting and Transfer of Plant Shoots

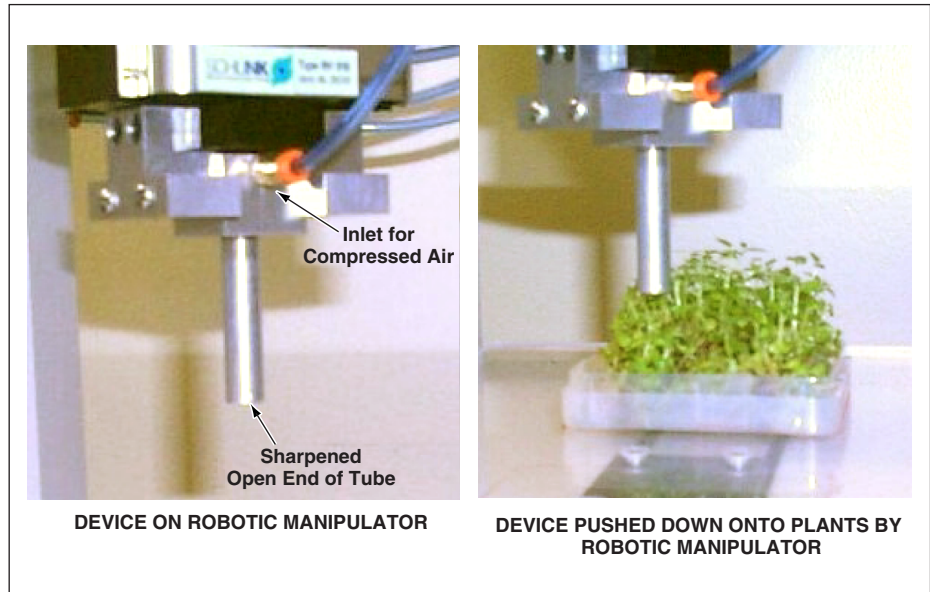
This device is simple yet effective.

NASA's Jet Propulsion Laboratory, Pasadena, California

A device that enables the automated cutting and transfer of plant shoots is undergoing development for use in the propagation of plants in a nursery or laboratory. At present, it is standard practice for a human technician to use a knife and forceps to cut, separate, and grasp a plant shoot. The great advantage offered by the present device is that its design and operation are simpler than would be those of a device based on the manual cutting/separation/grasping procedure. [The present device should not be confused with a prior device developed for partly the same purpose and described in "Compliant Gripper for a Robotic Manipulator" (NPO-21104), *NASA Tech Briefs*, Vol. 27, No. 3 (March 2003), page 59.]

The device (see figure) includes a circular tube sharpened at its open (lower) end and mounted on a robotic manipulator at its closed (upper) end. The robotic manipulator simply pushes the sharpened open end of the tube down onto a bed of plants and rotates a few degrees clockwise then counterclockwise about the vertical axis, causing the tube to cut a cylindrical plug of plant material. Exploiting the natural friction between the tube and plug, the tube retains the plug, without need for a gripping mechanism and control.

The robotic manipulator then retracts the tube, translates it to a new location over a plant-growth tray, and in-



Pushed Down Onto a Bed of Plants, the tube cuts and retains a plug of plant material. There is no need for separate cutting and grasping mechanisms and their controls.

serts the tube part way into the growth medium at this location in the tray. A short burst of compressed air is admitted to the upper end of the tube to eject the plug of plant material and drive it into the growth medium.

A prototype has been tested and verified to function substantially as intended. It is projected that in the fully developed robotic plant-propagation system, the robot control system would include a machine-vision subsystem that would automatically guide the robotic manipulator

in choosing the positions from which to cut plugs of plant material. Planned further development efforts also include more testing and refinement of the design and operation described above.

This work was done by Raymond Cipra, NASA Summer Faculty Fellow from Purdue University, Hari Das and Khaled Ali of Caltech, and Dennis Hong of Purdue University for NASA's Jet Propulsion Laboratory. Further information is contained in a TSP (see page 1). NPO-21137

Extension of Liouville Formalism to Postinstability Dynamics

A fictitious stabilizing force is introduced.

NASA's Jet Propulsion Laboratory, Pasadena, California

A mathematical formalism has been developed for predicting the postinstability motions of a dynamic system governed by a system of nonlinear equations and subject to initial conditions. Previously, there was no general method for prediction and mathematical modeling of postinstability behav-

iors (e.g., chaos and turbulence) in such a system.

The formalism of nonlinear dynamics does not afford means to discriminate between stable and unstable motions: an additional stability analysis is necessary for such discrimination. However, an additional stability analysis does not suggest

any modifications of a mathematical model that would enable the model to describe postinstability motions efficiently. The most important type of instability that necessitates a postinstability description is associated with positive Lyapunov exponents. Such an instability leads to exponential growth of small errors in initial

conditions or, equivalently, exponential divergence of neighboring trajectories.

The development of the present formalism was undertaken in an effort to remove positive Lyapunov exponents. The means chosen to accomplish this is coupling of the governing dynamical equations with the corresponding Liouville equation that describes the evolution of the flow of error probability. The underlying idea is to suppress the divergences of different trajectories that correspond to different initial conditions, without affecting a target trajectory, which is one that starts with prescribed initial conditions.

This formalism applies to a system of n first-order ordinary differential equations in n unknown dynamical variables:

$$\dot{x}_i = f_i[\mathbf{x}(t), t],$$

where i is an integer between 1 and n , x_i is one of the unknown dynamical variables, the overdot signifies differentiation with respect to time, \mathbf{x} is the vector of all the dynamical variables (x_1, x_2, \dots, x_n), and t is time. The prescribed initial conditions are given by

$$x_i(0) = x_i^0$$

The corresponding Liouville equation for the evolution of the probability distribution of errors in the initial conditions is

$$\partial\rho/\partial t + \nabla \cdot (\rho\mathbf{f}) = 0$$

where \mathbf{f} is the vector of all the forcing functions (f_1, f_2, \dots, f_n). It is assumed that this probability distribution peaks at zero error (representing the prescribed initial conditions). A fictitious stabilizing force proportional to the gradient of the probability density in the space of the dynamical variables is added to the system of differential equations, yielding the following system of modified dynamical equations:

$$\dot{x}_i = f_i + h_0 \partial\rho/\partial x_i,$$

where $\rho(\mathbf{x}(t))$ is the probability distribution and h_0 is an arbitrary factor of proportionality. The corresponding modified Liouville equation is

$$\partial\rho/\partial t + \nabla \cdot [\rho(\mathbf{f} + h_0\nabla\rho)],$$

The stabilizing potential $h_0\rho$ creates a powerful attractor that corresponds to the occurrence of the target trajectory with probability one.

Because the modified Liouville equation does not depend on the modified

dynamical equations, the modified Liouville equation can be solved in advance, so that the stabilizing force becomes a known function. The modified Liouville equation is solved subject to a normalization constraint and to an initial condition (an initial probability distribution) that can be specified somewhat arbitrarily. The initial condition can be, for example, a product of analysis of errors in previous dynamical computations.

An application of this formalism to Hamiltonian dynamics leads to a demonstration of a formal similarity between the stabilizing potential and a quantum potential that appears in the Madelung form of the Schroedinger equation of a single particle. Although physical meaning of the quantum potential is not completely understood, loosely speaking, it can be interpreted as a mechanism for enforcement of the uncertainty relationship that bounds the precision with which positions and velocities can be observed.

*This work was done by Michail Zak of Caltech for NASA's Jet Propulsion Laboratory. Further information is contained in a TSP (see page 1).
NPO-30393*

Advances in Thrust-Based Emergency Control of an Airplane

It should be possible to land safely after a primary-flight-control failure.

Dryden Flight Research Center, Edwards, California

Engineers at NASA's Dryden Flight Research Center have received a patent on an emergency flight-control method implemented by a propulsion-controlled aircraft (PCA) system. Utilizing the pre-existing auto-throttle and engine-pressure-ratio trim controls of the airplane,

the PCA system provides pitch and roll control for landing an airplane safely without using aerodynamic control surfaces that have ceased to function because of a primary-flight-control-system failure. The installation of the PCA does not entail any changes in pre-existing

engine hardware or software. [Aspects of the method and system at previous stages of development were reported in "Thrust-Control System for Emergency Control of an Airplane" (DRC-96-07), *NASA Tech Briefs*, Vol. 25, No. 3 (March 2001), page 68 and "Emergency Land-

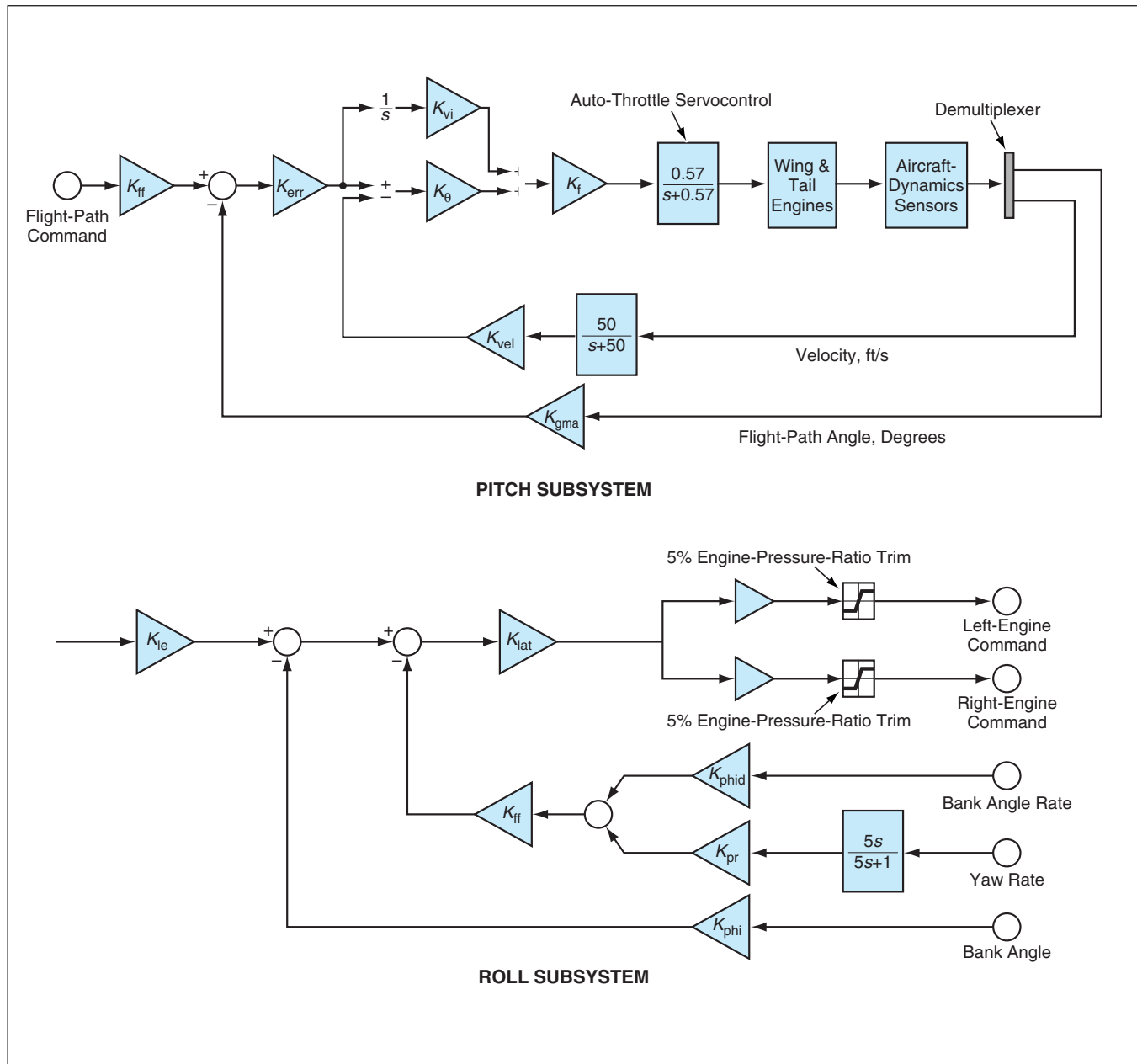


Figure 1. These Emergency Propulsion Control Subsystems are combined to obtain the PCA. The pitch subsystem utilizes the auto-throttle to control the pitch or the flight-path angle. The roll subsystem utilizes a five-percent engine trim feature.

ing Using Thrust Control and Shift of Weight" (DRC-96-55), *NASA Tech Briefs*, Vol. 26, No. 5 (May 2002), page 58.]

Aircraft flight-control systems are designed with extensive redundancy to ensure low probabilities of failure. During recent years, however, several airplanes have exhibited major flight-control-system failures, leaving engine thrust as the last mode of flight control. In some of these emergency situations, engine thrusts were successfully modulated by the pilots to maintain flight paths or pitch angles, but in other situations, lateral control was also needed. In the majority of such control-system failures, crashes resulted and over 1,200 people died.

The challenge lay in creating a means of sufficient degree of thrust-modulation control to safely fly and land a stricken airplane. A thrust-modulation control system designed for this purpose was flight-tested in a PCA — an MD-11 airplane. The results of the flight test showed that without any operational control surfaces, a pilot can land a crippled airplane (U.S. Patent 5,330,131). The installation of the origi-

nal PCA system entailed modifications not only of the flight-control computer (FCC) of the airplane but also of each engine-control computer. Inasmuch as engine-manufacturer warranties do not apply to modified engines, the challenge became one of creating a PCA system that does not entail modifications of the engine computers.

The present PCA system, discussed in U.S. Patents 6,102,330 and 6,041,273, provides longitudinal and lateral (pitch and roll) control, effected solely by modifications of the software of pre-existing flight-control computers, and without any changes in the engine controller or any hardware changes in the cockpit. In the event of a failure in the primary-flight-control system, the engines can be used to dampen unwanted motion, enabling a safe landing. This method eliminates the longitudinal and roll-control tasks. The combination of the teachings of the two patents enables a pilot to align airplane with a runway and land in a normal fashion.

The upper part of Figure 1 shows a pitch- (or flight-path-angle) command subsystem that utilizes feedback from a

velocity sensor and a flight-path angle (g) sensor. The pilot controls an auto-throttle propulsion subsystem by use of a thumbwheel. The signals from this pitch- (or flight-path-angle) command subsystem drive an auto-throttle servo-control forward or backward, thereby causing the engines to increase or decrease thrust, and thereby further controlling the pitch of the airplane. This control action keeps the phugoid mode well damped. Auto-throttle systems are already installed in many multi-engine aircraft, eliminating the need for hardware changes to take advantage of this control action.

The lower part of Figure 1 shows a roll/lateral-axis command subsystem that enables the pilot to turn or roll the airplane down to the runway. The signal that drives the roll-control subsystem comes from a heading knob in the cockpit. By combining the subsystems of Figure 1, one obtains a total PCA system that can be installed and operated without need to modify engine hardware or software. The benefits of utilizing this PCA system include smaller (in comparison to a system that involves engine modifications) development costs and continued viability of the original engine warranties.

The combination of the pitch and roll subsystems of Figure 1 enables a pilot to control a crippled airplane in a manner comparable to that of landing a healthy airplane. Figure 2 shows some expected responses of a wide body airplane flown with engines-only control by use of the PCA system. The auto-throttle emergency PCA system controls the airplane with good damping of pitching motion. The flight-path angle pitches up 1° and tracks the command very well. The thrust is increased and decreased automatically to control the pitching motion. At the same time, the roll angle is commanded to 10° to the right: The roll angle is made to go to 10° in a time of ≈20 s by use of lateral engine pressure-ratio trim control, with an increase in power of the left engine and a decrease in power of the right engine.

This work was done by Gray Creech, John J. Burken, and Bill Burcham of Dryden Flight Research Center. Further information is contained in a TSP (see page 1).

This invention has been patented by NASA (U.S. Patent No. 6,102,330). Inquiries concerning nonexclusive or exclusive license for its commercial development should be addressed the Patent Counsel, Dryden Flight Research Center; (805) 258-3720. Refer to DRC-97-21.

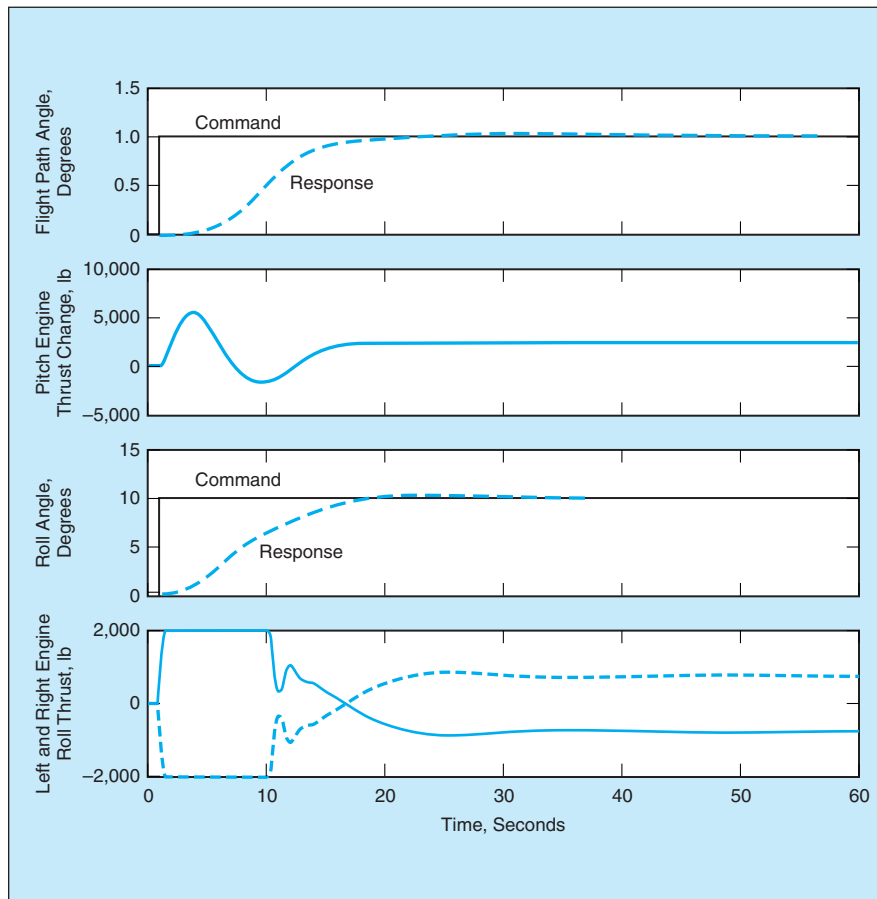


Figure 2. These **Dynamic Responses** to a flight-path angle command of 1° and a simultaneous roll command of 10° were computed for an MD-11 airplane, the weight of each wing-mounted engine of which was considered to be increased by 5,000 lb (≈2.3 tonnes).

Ultrasonic/Sonic Mechanisms for Drilling and Coring

These mechanisms imitate burrowing actions of gophers and crabs.

NASA's Jet Propulsion Laboratory, Pasadena, California

Two apparatuses now under development are intended to perform a variety of deep-drilling, coring, and sensing functions for subsurface exploration of rock and soil. These are modified versions of the apparatuses described in "Ultrasonic/Sonic Drill/Corers With Integrated Sensors" (NPO-20856), *NASA Tech Briefs*, Vol. 25, No. 1 (January 2001), page 38. In comparison with the drilling equipment traditionally used in such exploration, these apparatuses weigh less and consume less power. Moreover, unlike traditional drills and corers, these apparatuses function without need for large externally applied axial forces.

To recapitulate from the cited prior article: An apparatus of this type is an approximately cylindrical shaped vehicle that contains driving and controlling electronic circuits plus sensors and associated electronic circuitry. The vehicle also contains an electronically driven piezoelectric actuator that excites a combination of ultrasonic and sonic vibrations that give rise to hammering action at a tip that, as a result of this action, advances through the soil, rock, or other material in which it is embedded. The combination of ultrasonic and sonic vibrations is more effective for drilling than is the microhammering action of ultrasonic vibrations alone. Unlike in conventional twist drilling, a negligible amount of externally applied axial force is needed to make the apparatus advance through the material. Because there are transverse vibrations as well as longitudinal ones, a hole somewhat wider than the apparatus is formed; consequently, unlike in the case of a conventional twist drill, there is resistance to jamming and tolerance of misalignment.

Each of the present developmental apparatuses is denoted an ultrasonic/sonic mechanism of deep drilling (USMOD). In each USMOD, a hollow cylindrical piezoelectric actuator vibrates an inverted horn that impinges on a bobbin-shaped free mass. In addition to serving as a linkage between the horn and a drilling or coring bit, the free mass also functions as a frequency transformer, producing the low-frequency hammering action. The drilling or coring bit has an outside diameter about equal to or greater than that of the actuator. Tan-

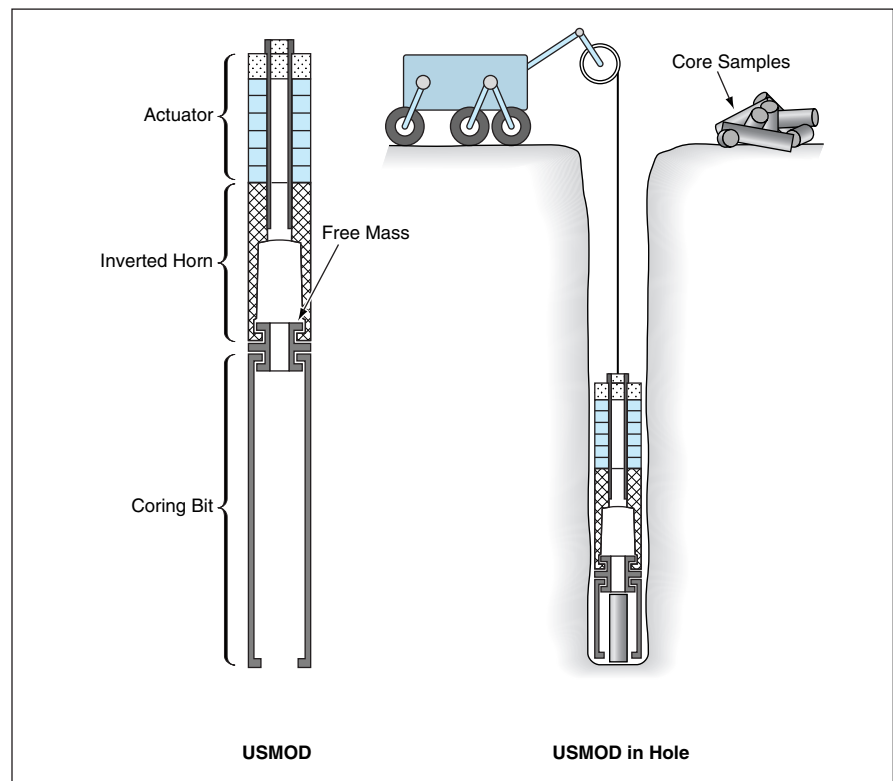


Figure 1. The **Ultrasonic Gopher** advances into the ground as a result of vibrations of its coring bit. Periodically, the apparatus is lifted out of the hole by use of a cable to extract a core sample.

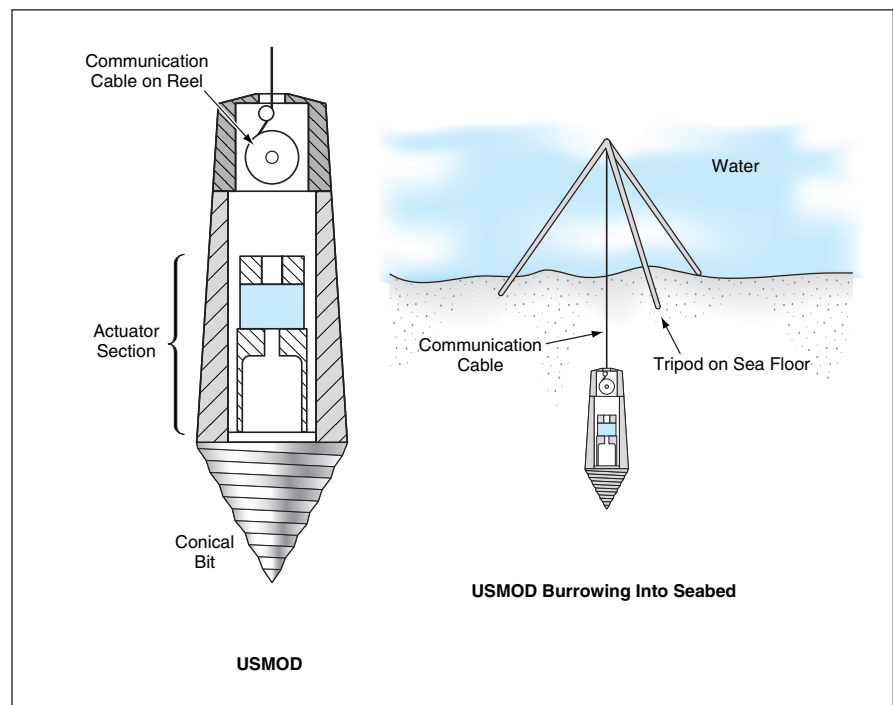


Figure 2. The **Ultrasonic Crab** burrows, without leaving an open hole behind. To enable communication with a surface unit, it pays out a cable as it moves through the ground.

gential forces generated by actuation of the drilling or coring bit are expected not only to prevent jamming but also to be exploitable for simple steering. The cavity inside the actuator and horn sections contains packages of electronic circuitry and possibly some or all sensors.

Both USMODs are designed to drill to depths much greater than their lengths. One USMOD (see Figure 1) is intended for use mainly in acquiring cores. It is denoted an ultrasonic gopher because, like a gopher, it periodically stops advancing at the end of the hole to bring excavated material (in this case, a core sample) to the surface, then re-enters

the hole to resume the advance of the end of the hole. By use of a cable suspended from a reel on the surface, this USMOD is lifted from the hole to remove a core sample, then lowered into the hole to resume the advance and acquire the next core sample.

The other USMOD (see Figure 2) is intended to perform sensing at a desired depth. Instead of a cylindrical coring bit, this USMOD is equipped with a conical drilling bit. This USMOD is denoted an ultrasonic crab because, like a sand crab, it burrows by rapidly shaking its body. Unlike the ultrasonic gopher, this one does not acquire samples or leave an

open hole behind itself: instead, debris from drilling are pushed behind this USMOD as it advances, closing the hole behind it. A wire for communication with a surface unit is unwound from a reel in a rear compartment as this USMOD advances through the ground.

*This work was done by Yoseph Bar-Cohen, Stewart Sherrit, and Benjamin Dolgin of Caltech and Steve Askin, Thomas M. Peterson, Bill Bell, Jason Kroh, Dharmendra Pal, Ron Krahe, and Shu Du of Cybersonics for NASA's **Jet Propulsion Laboratory**. Further information is contained in a TSP (see page 1).
NPO-30291*



Exercise Device Would Exert Selectable Constant Resistance

Lyndon B. Johnson Space Center, Houston, Texas

An apparatus called the resistive exercise device (RED) has been proposed to satisfy a requirement for exercise equipment aboard the International Space Station (ISS) that could passively exert a selectable constant load on both the outward and return strokes. The RED could be used alone; alternatively, the RED could be used in combination with another apparatus called the treadmill with vibration isolation and stabilization (TVIS), in which case the combination would be called the subject load device

(SLD). The basic RED would be a passive device, but it could incorporate an electric motor to provide eccentric augmentation (augmentation to make the load during inward movement greater than the load during outward movement). The RED concept represents a unique approach to providing a constant but selectable resistive load for exercise for the maintenance and development of muscles. Going beyond the original ISS application, the RED could be used on Earth as resistive weight

training equipment. The advantage of the RED over conventional weight-lifting equipment is that it could be made portable and lightweight.

*This work was done by Damon C. Smith of Lockheed Martin for **Johnson Space Center**.*

This invention is owned by NASA, and a patent application has been filed. Inquiries concerning nonexclusive or exclusive license for its commercial development should be addressed to the Patent Counsel, Johnson Space Center, (281) 483-0837. Refer to MSC-23196.



Improved Apparatus for Measuring Distance Between Axles

Accuracy is double that of the previous version.

John F. Kennedy Space Center, Florida

An improved version of an optoelectronic apparatus for measuring distances of the order of tens of feet with an error no larger than a small fraction of an inch (a few millimeters) has been built. Like the previous version, the present improved version of the apparatus is designed to measure the distance ≈ 66 ft (≈ 20 m) between the axes of rotation of the front and rear tires of the space shuttle orbiter as it rests in a ground-based processing facility. Like the previous version, the present version could also be adapted for similar purposes in other settings: Examples include measuring perpendicular distance from a wall in a building, placement of architectural foundations, and general alignment and measurement operations.

The previous version was described in "Apparatus and Technique for Measuring Distance Between Axles" (KSC-11980), *NASA Tech Briefs*, Vol. 25, No. 3 (March 2000), page 76. To recapitulate: The major components of the apparatus were (1) a laser range finder and (2) laser line projectors that included two battery-powered laser-diode modules with collimating optics. Each laser-diode module generated a continuous-wave beam with a power of 3 mW at a wavelength of 670 nm. The modules were aimed to point the beams downward, and the beams were made to pass

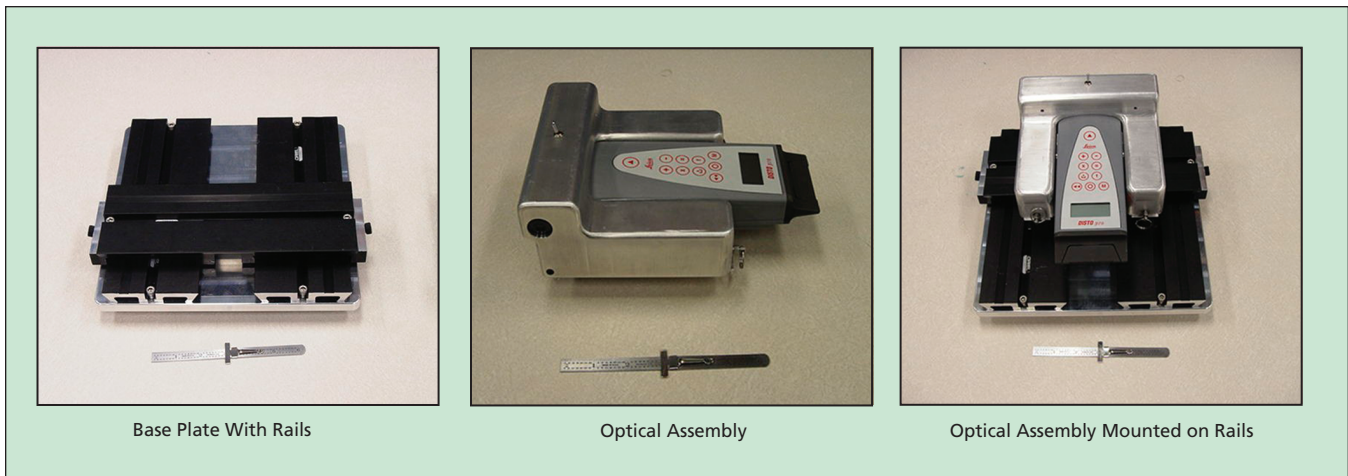
through cylindrical diverging lenses to spread the beams into fans oriented in a nominally vertical plane. The modules were aligned to project coincident vertical lines as viewed from the side and collinear horizontal lines as viewed from the top.

The range finder was aligned precisely with respect to the laser-diode modules and the diverging lenses so that the line of sight of the range finder was perpendicular to the plane defined by the beams from the laser-diode modules. This line of sight was thus nominally horizontal. The apparatus was mounted on a tripod (between the rear tires, in the case of a space shuttle) with the range finder at approximately the height of the distant object of interest (the front tire hub in the case of the space shuttle). Exact matching of heights was not necessary in this application because the geometry was such that even at a height difference as large as a few inches, the difference between the horizontal distance and the measured distance was less than the allowable error of $1/8$ in (≈ 3.2 mm). A target was mounted on the distant object of interest (the front tire hub). The position and orientation of the apparatus were adjusted until the bright lines projected by the fan beams struck the near objects of interest (the hubs of both rear tires in the space-shuttle applica-

tion) and the beam from the range finder struck the center of the target. Then the distance was measured by use of the range finder, which produced a digital readout. The measurement range was from <1 ft (<0.3 m) to about 300 ft (≈ 91 m).

The differences between the previous and present versions are the following:

- In the previous version, an optical assembly containing the laser fan-beam generators and the laser range finder was aligned by sliding it on top of a platform attached to a tripod. Because this alignment process proved awkward in practice, rails were added so that the optical assembly could be aligned more precisely and then locked in position. As shown in the left part of the figure, there are two pairs of parallel rails for left/right motion of the assembly and a single rail for forward/backward motion of the assembly.
- The original range finder was replaced with a newer and more accurate one, reducing the measurement error to within a tolerance of $1/16$ in. (≈ 1.6 mm).
- Rechargeable batteries that were used in the original version were found to last only a couple of years. They were replaced by batteries of common non-rechargeable AA-size cells.
- The original tripod was replaced with a more rugged one.
- Hinged plates with simple pull pins



Parts of the Improved Distance-Measuring Apparatus are shown here, variously, by themselves and assembled with other parts. [A ruler in each photo is approximately 6 in. (15 cm) long.]

were installed to afford access, for replacing batteries without need to use tools.

- In the previous version, it was necessary to cut cylindrical lenses and glue them to the laser diodes. During the last few intervening years, much better

laser devices arrived on the market. Therefore, the original laser diodes were replaced by laser-diode assemblies that include built-in adjustable focus devices so that the projected lines can be made narrow, increasing the accuracy of apparatus.

This work was done by Douglas E. Willard of Kennedy Space Center and Ivan I. Townsend III of Dynacs, Inc. For further information, contact the Kennedy Technology Programs and Commercialization Office at (321) 867-8130. KSC-12391

Six Classes of Diffraction-Based Optoelectronic Instruments

These instruments can play diverse roles in scientific instrumentation.

Ames Research Center, Moffett Field, California

Six classes of diffraction-based optoelectronic instruments have been invented as means for wavelength-based processing of light. One family of anticipated applications lies in scientific instrumentation for studying chemical and physical reactions that affect and/or are affected differently by light of different wavelengths or different combinations of wavelengths. Another family of anticipated applications lies in optoelectronic communication systems.

An instrument of the first class is basically a spectrometer that can serve as a building block for the instruments of the other classes. In this instrument, a beam of light emitted from the site of a chemical or physical reaction strikes a diffraction grating, which causes each of its wavelength components to propagate in a direction that depends on its wavelength. Photodetectors are positioned to receive light diffracted to different angular intervals that, by virtue of the aforementioned diffraction, correspond to different wavelength bands. Hence, the photodetector outputs are indicative of the time-dependent intensities of light emitted by the chemical or physical reaction in the selected wavelength bands.

In an instrument of the second class, the input light comprises two beams. In one of two possible modes of operation, the purpose served by the instrument is to help determine whether the beams are correlated sufficiently to be considered as having originated from the same source. In the other mode of operation, one of the beams is a reference beam and the instrument is used to compare the other beam with the reference beam. The two

incoming beams impinge from different directions on a diffraction grating. As in the first instrument, the diffracted light from each beam impinges on photodetectors corresponding to various wavelength bands. In this case, there are two sets of photodetectors — one for each incoming beam. The outputs of the photodetectors as functions of time are sampled and the samples used to compute correlations between the time-dependent spectra of the two beams. The correlation values are taken to be indications of the relatedness or unrelatedness of the incoming beams.

In an instrument of the third class, a beam of light is split into two beams, which are then diffracted into wavelength components. One set of wavelength-component beams passes through a chamber containing a medium (hereafter denoted the altered medium) that could be undergoing a reaction that one seeks to study. The other set of wavelength-component beams passes through an otherwise identical chamber that contains a reference medium. After passage through the chambers, the two sets of wavelength-component beams impinge on photodetectors that are arranged in one or two sets, depending on the number and arrangement of diffraction gratings. The outputs of the photodetectors are sampled and processed to analyze differences between the effects of the altered and reference media on the light propagating through them.

The instruments of the fourth class can exist in diverse forms. Common to all forms is the use of diffraction gratings to split beams of light from multiple sources into wavelength components, which are

then made to impinge on reaction sites to determine whether light at those wavelengths does or does not promote the reactions in question. In some cases reactions may be promoted by light of different wavelengths impinging in specified sequences within short intervals of time; the instruments of this class can be designed to generate the required sequences and measure their effects.

An instrument of the fifth class includes two coaxial cylinders. The outer surface of the inner cylinder is covered with a diffraction grating. The outer cylinder holds an array of photodetectors that intercept light diffracted by the grating. The cylinders can be translated axially and/or rotated, relative to each other, to change the wavelength range of the monitored light.

An instrument of the sixth class is a beam-steering device for data communication. A light beam modulated to convey symbols impinges successively on two diffraction gratings. The direction(s) of diffraction depend(s) on the wavelength(s) present in the beam. Hence, diffraction can be used to steer the beam, according to its wavelength, to one or more desired photodetector(s) in an array.

This work was done by Stevan Spremo of Ames Research Center, Peter Fuhr of San Jose State University Foundation, and John Schipper, Law Offices of John Schipper. Further information is contained in a TSP (see page 1).

Inquiries concerning rights for the commercial use of this invention should be addressed to the Patent Counsel, Ames Research Center, (650) 604-5104. Refer to ARC-14650.



Modernizing Fortran 77 Legacy Codes

The investment in established codes is preserved as modern capabilities are added.

NASA's Jet Propulsion Laboratory, Pasadena, California

An incremental approach to modernization of scientific software written in the Fortran 77 computing language has been developed. This approach makes it possible to preserve the investment in legacy Fortran software while augmenting the software with modern capabilities to satisfy expanded requirements. This approach could be advantageous (1) in situations in which major rewriting of application programs is undesirable or impossible, or (2) as a means of transition to major rewriting.

Programs written in Fortran 77 and other early versions of Fortran retain much intellectual and commercial value. These codes have been carefully validated and often perform excellently, even on modern computers. However, the early versions of Fortran are often not adequate for the increasingly complex systems typically encountered in current practice. For example, early Fortran programs may not utilize dynamic memory or their data structures may not reflect problem domains well. Often, user interfaces are poor or nonexistent. On the other hand, modern programming languages (most notably, object-oriented languages) offer much better support for complex programming projects.

The developers of the present incremental approach have found that con-

trary to the conventional wisdom among object-oriented programmers, it is not necessary to redesign codes from the bottom up to make them object-oriented. Many object-oriented programs make use of non-object-oriented libraries for basic functions — for example, calling operating systems. The important question in modernization of a legacy code is whether the subroutines in the code have sufficient basic functionality. For most legacy codes that have been in use for a decade or more, this is the case. The weaknesses of legacy codes arise with respect to flexibility, extensibility, and related issues.

The present incremental approach is based partly on the assumption that such weaknesses can be addressed at a higher level, by building interface software libraries that mediate between main programs and underlying legacy codes. Major goals in this approach are to increase program safety, simplify interfaces to subroutines, add dynamic memory management, encapsulate different parts of programs, add abstract data types that reflect the problem domains, and add or improve user interfaces.

The present incremental approach can be characterized as one of building modern superstructures around legacy codes rather than completely rewriting those codes. Building such a superstruc-

ture increases the opportunity to reuse the intellectual capital already invested in the legacy code and entails less risk that the rewrite might not work properly. As much as possible, one avoids modification of original subroutines; instead, one strives to embed the modern features in an interface library.

This approach admits of several methodologies. One such methodology is based on Fortran 90, because this language has modern features yet maintains compatibility with older Fortran software. Other methodologies could be based on other modern computing languages (for example, C++) in which one can write programs capable of calling the original Fortran subroutines. Once software constructed following this approach works correctly, there is always the option of replacing individual pieces of the legacy code, and eventually even the entire code. One important advantage of the use of a software superstructure is that the legacy code can still be used during a modernization effort.

This work was done by Viktor Decyk and Charles Norton of Caltech for NASA's Jet Propulsion Laboratory. Further information is contained in a TSP (see page 1).

This software is available for commercial licensing. Please contact Don Hart of the California Institute of Technology at (818) 393-3425. Refer to NPO-21166.

Active State Model for Autonomous Systems

Autonomous systems would be able to diagnose themselves and respond accordingly.

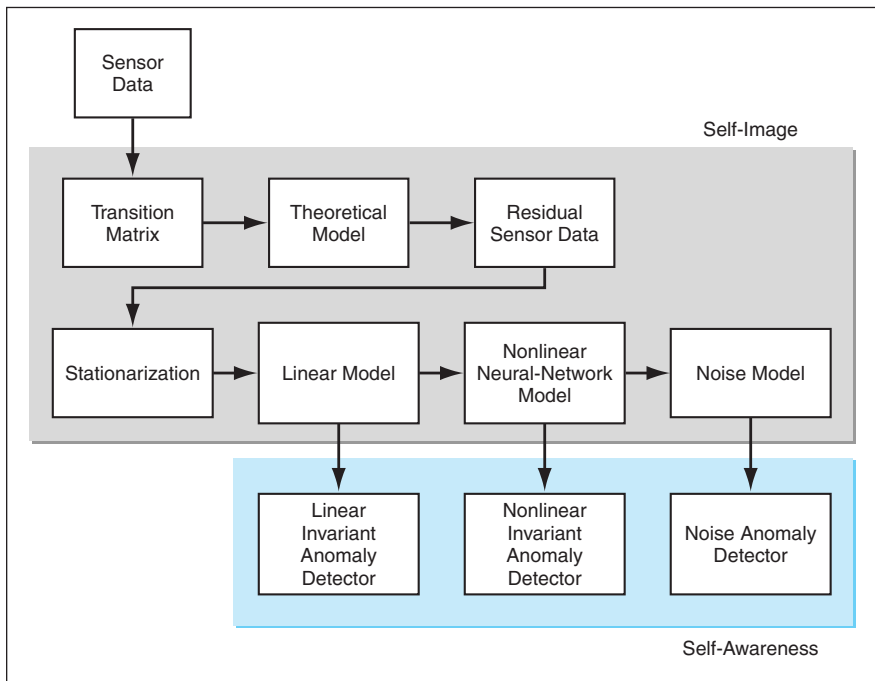
NASA's Jet Propulsion Laboratory, Pasadena, California

The concept of the active state model (ASM) is an architecture for the development of advanced integrated fault-detection-and-isolation (FDI) systems for robotic land vehicles, pilotless aircraft, exploratory spacecraft, or other complex engineering systems that will be capable of autonomous operation. An FDI system based on the ASM concept would not only provide traditional diagnostic

capabilities, but also integrate the FDI system under a unified framework and provide mechanism for sharing of information between FDI subsystems to fully assess the overall "health" of the system.

The ASM concept begins with definitions borrowed from psychology, wherein a system is regarded as active when it possesses self-image, self-awareness, and an ability to make decisions itself, such that

it is able to perform purposeful motions and other transitions with some degree of autonomy from the environment. For an engineering system, self-image would manifest itself as the ability to determine nominal values of sensor data by use of a mathematical model of itself, and self-awareness would manifest itself as the ability to relate sensor data to their nominal values. The ASM for such a system



This **Flow Chart** depicts stages of computation in the gray-box approach to self-image and self-awareness of a complex engineering system.

may start with the closed-loop control dynamics that describe the evolution of state variables. As soon as this model was supplemented with nominal values of sensor data, it would possess self-image. The ability to process the current sensor data and compare them with the nominal values would represent self-awareness. On the basis of self-image and self-awareness, the ASM provides the capability for self-identification, detection of abnormalities, and self-diagnosis.

In our practical implementation of the ASM, we use the “gray-box” approach to implementing self-image and self-aware-

ness (see figure). The “gray-box” approach differs from the “black-box” and “white-box” approaches in the following way: It involves the use of mathematical models that are characterized as being of a mixed-signal or “gray” type, meaning that they include both deterministic and stochastic models. The deterministic or the “white” model is used to filter out what is known about the system. What is left after filtering is the residual, or unknown, components of information on the system. The residual information is mathematically modeled by use of stochastic techniques, i.e., “black-box.” The

behavior or “health” of the system can then be monitored by comparing the residual against its nominal values through the stochastic model. The advantages of the gray-box approach are that (1) it maximizes the use of both sensory information and any information previously available in the form of a mathematical model and (2) offers both sensitivity to truly functional damage and insensitivity to mere operational disturbances.

Another essential component of the ASM is the active system exchange (ASE), which includes a flexible database that stores all relevant FDI and other information to synthesize data and data-driven models sufficient for intelligent decision-making. The ASE would provide crucial information from all FDI subsystems and would allow an intelligent agent such as planning software to make decisions based on summarized understanding of the system health. When the full ASM architecture is implemented, it will provide a framework for a fully autonomous system that would be able to monitor and predict equipment failures, reconfigure the control subsystem of the system in response to an equipment failure, take appropriate action in response to unexpected events, and replan the mission of the system, as needed, in real time.

This work was done by Han Park, Steve Chien, Michail Zak, Mark James, Ryan Mackey, and Forest Fisher of Caltech for NASA’s Jet Propulsion Laboratory. Further information is contained in a TSP (see page 1).

NPO-21243



⊕ Shields for Enhanced Protection Against High-Speed Debris

A report describes improvements over the conventional Whipple shield (two thin, spaced aluminum walls) for protecting spacecraft against high-speed impacts of orbiting debris. The debris in question arise mainly from breakup of older spacecraft. The improved shields include exterior “bumper” layers composed of hybrid fabrics woven from combinations of ceramic fibers and high-density metallic wires or, alternatively, completely metallic outer layers composed of high-strength steel or copper wires. These shields are designed to be light in weight, yet capable of protecting against orbital debris with mass densities up to about 9 g/cm^3 , without generating damaging secondary debris particles. As yet another design option, improved shields can include sparsely distributed wires made of shape-memory metals that can be thermally activated from compact storage containers to form shields of predetermined shape upon arrival in orbit. The improved shields could also be used to augment shields installed previously.

This work was done by Eric L. Christiansen and Justin H. Kerr of Johnson Space Center. Further information is contained in a TSP (see page 1).

This invention is owned by NASA, and a patent application has been filed. Inquiries concerning nonexclusive or exclusive license for its commercial development should be addressed to the Patent Counsel, Johnson Space Center, (281) 483-0837. Refer to MSC-23443.

⊕ Scaling of Two-Phase Flows to Partial-Earth Gravity

A report presents a method of scaling, to partial-Earth gravity, of parameters that describe pressure drops and other characteristics of two-phase (liquid/vapor) flows. The development of the method was prompted by the need for a means of designing two-phase flow systems to operate on the Moon and on Mars, using fluid-properties and flow data from terrestrial two-phase-flow experiments, thus eliminating the need for partial-gravity testing. The report presents an explicit procedure for designing an Earth-based test bed that can provide hydrodynamic similarity with two-phase fluids flowing in partial-gravity systems. The procedure does not require prior knowledge of the flow regime (i.e., the spatial orientation of the phases). The method also provides for determination of pressure drops in two-phase partial-gravity flows by use of a generalization of the classical Moody chart (previously applicable to single-phase flow only). The report presents experimental data from Mars- and Moon-activity experiments that appear to demonstrate the validity of this method.

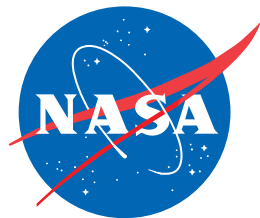
This work was done by Kathryn M. Hurlbert of Johnson Space Center and Larry C. Witte of the University of Houston. Further information is contained in a TSP (see page 1).

MSC-23319

⊕ Neutral-Axis Springs for Thin-Wall Integral Boom Hinges

A document proposes the use of neutral-axis springs to augment the unfolding torques of hinges that are integral parts of thin-wall composite-material booms used to deploy scientific instruments from spacecraft. A spring according to the proposal would most likely be made of metal and could be either flat or curved in the manner of a measuring tape. Under the unfolded, straight-boom condition, each spring would lie along the neutral axis of a boom. The spring would be connected to the boom by two supports at fixed locations on the boom. The spring would be fixed to one of the supports and would be free to slide through the other support. The width, thickness, and material of the spring would be chosen to tailor the spring stiffness to provide the desired torque margin to assist in deployment of the boom. The spring would also contribute to the stiffness of the boom against bending and torsion, and could help suppress unwanted vibrations caused by the deployment process or by external disturbances.

This work was done by James M. Ryan of Goddard Space Flight Center. Further information is contained in a TSP (see page 1). GSC-14640



National Aeronautics and
Space Administration